

## In-silico screening of potential targets from wound healing pathways against Hordenine and selected Bioisostere

<sup>1</sup> S.Amsaveni, <sup>2</sup>S.Radha Mahendran, <sup>3</sup> G.Surya, <sup>4</sup>Umashankar Vetrivel <sup>5</sup> Luke Elizabeth Hanna

<sup>1,2,3</sup>Department of Bioinformatics, School of Life Sciences,Vels Institute of Science, Technology and Advanced Studies (VISTAS), Pallavaram, Chennai

<sup>4,5</sup>Department of Virology and Biotechnology, ICMR-National Institute for Research in Tuberculosis, Chetpet, Chennai

**Corresponding author: S.Amsaveni amsvet1982@gmail.com**

### KEYWORDS

Wound healing, Autodock 4.0, Bioisostere, ADMET, MD simulations, PLIP

### ABSTRACT

Hordenine (4-[2-(Dimethylamino) ethyl] phenol) a plant-based phenethylamine alkaloid and its shortlisted bioisostere 1-(5-amino-1H-1,2,4-triazol-3-yl)-N-[2-(4-chlorophenyl) ethyl]-N-methylpiperidin-4-amine, which showed nil-lead likeliness violation during ADMET screening were docked with eight potential drug targets from selected wound healing pathways. The results showed that Metalloproteinase-9 and Proliferating cell antigen had the lowest binding energy of -6.23 and -6.58 kcal/mol, respectively. However, when considering the molecular interactions were considered, Tyrosine related protein 1 had the maximum number of interactions with binding energy of -5.83 kcal/mol and the highest number of hydrogen bonds. The molecule 1-(5-amino-1H-1,2,4-triazol-3-yl)-N-[2-(4-chlorophenyl)ethyl]-N-methylpiperidin-4-amine docked well with all the targets and had appreciably lower binding energies for all the wound healing targets: Casein kinase 1 -14.41Kcal/mol, Metalloproteinase-9 -11.7241Kcal/mol, Proliferating cell antigen -9.8941Kcal/mol, Tyrosine related protein 1 -9.4441Kcal/mol,  $\beta$ 2 adrenergic receptors -8.1941Kcal/mol, Notch1 I D receptor -7.4441Kcal/mol, Dopachrome tautomerase -6.441Kcal/mol and Glycogen synthase kinase 3 beta -5.741Kcal/mol. The Molecular dynamic simulations of Casein kinase 1 with 1-(5-amino-1H-1,2,4-triazol-3-yl)-N-[2-(4-chlorophenyl) ethyl]-N-methylpiperidin-4-amine showed that the  $\alpha$  Root mean square deviation values were within 1.6 Å throughout the simulation for the system and the root mean square fluctuations showed that loop residues (Residues 49 to 57) involved in ligand binding had minimal fluctuations as compared to the other loop residues. A free binding energy of -10.44 Kcal /mol was derived from MMPBSA calculations and this corroborated well with the good binding score obtained by docking. This shows that the protein-ligand complex did not undergo any major conformational change and was stable throughout the simulation giving supportive evidence that this molecule could be a promising candidate for acute and chronic wound healing including diabetic foot ulcers, along with Hordenine which is an effective inhibitor of hyperpigmentation.

## Introduction

Wound repair is a highly complex biological process [1] by which tissues restore normal function and architecture following any of a variety of physical, mechanical, biological, or chemical insults [2,3]. The process of acute wound healing is triggered by tissue injury and consists of a cascade of highly coordinated phases including hemostasis, inflammation, proliferation, and remodeling [4,5,6]. The healing process can be arrested in any of these phases, leading to the formation of a chronic non-healing wound [7]. Enhanced wound healing mechanisms can help in quick effective healing, despite the presence of risk factors that could result in chronic wounds [8].

## Acute Wounds

Tyrosine metabolism is a key pathway in the initial stage of healing of acute wounds [9]. Tyrosinase, which converts tyrosine to dopaquinone, is the key enzyme involved in the rate-limiting step of tyrosine metabolism, and Tyrosine related protein 1 (TYRP1) is an important melanosomal enzyme belonging to the Tyrosinase (TYR) family [10,11,12]. Dopachrome Tautomerase (DCT) is an important paralog of TYRP1 [13]. DCT and TYRP1 are both Hub and key functional genes and significant down-regulation of these enzymes in acute wound samples has been documented [9].

$\beta$ 2 adrenergic receptors ( $\beta$ 2-ARs) are found in high levels on keratinocytes play a role in cutaneous homeostasis [14,15,16]. Aberrations in either keratinocyte  $\beta$ 2-AR function or density have been associated with various skin diseases [14]. Upon injury, keratinocytes migrate directionally into the wound bed to initiate re-epithelialization which is essential for wound repair and restoration of the integrity of the skin barrier [17]. Keratinocytes express high level of ERK protein which plays an important role in keratinocyte migration [18,19,20,21]. Blockade of  $\beta$ 2-AR by an antagonist prevents endogenously synthesized catecholamine (Epinephrine) from binding, thus negating its anti-mitogenic effect and consequently accelerating wound repair [14, 22, 23].

The Wnt/ $\beta$ -catenin pathway improves angiogenesis and epithelial remodeling that are involved in the regulation of wound healing [24,25,26]. Casein kinase 1 (CK1) and Glycogen synthase kinase 3 beta (GSK3B) bind to their targets in the Wnt/ $\beta$ -catenin signalling pathway and act as positive regulators leading to increased signaling and eventually in effective wound healing process [27,28]. Activation of the Wnt pathway has a key role in fibroblast activation and collagen release during fibrosis. In the “off” state,  $\beta$ -catenin binds with GSK3 $\beta$ , axin2, adenomatous colon polyposis protein (APC), and CK-1 [29, 30]. The kinase in this complex phosphorylates-catenin,

thereby targeting to degradation of the ubiquitin proteasome system. On the other hand, in the on” state, the receptor complex consisting of Frizzled and LRP5/6 protein binds to Wnt, and recruits Disheveled Protein (DVL) to the plasma membrane. Subsequently, several components of the  $\beta$ -catenin destruction complex are recruited to the membrane, and they prevent the phosphorylation of  $\beta$ -catenin, which in turn stimulates the transcription of Wnt target genes such as cyclin D1, c-myc, and Axin2 resulting in events like cell division, cell proliferation and cell migration to the wound site [31,32, 33].

### **Inflammatory and proliferation phase**

p21, a potent cyclin dependent kinase (CDK) inhibitor which is a downstream protein of P53 regulates fibroblast cell proliferation and differentiation and increases wound healing[34,35]. [36,37]. The binding of p21 to the proliferating cell nuclear antigen (PCNA) causes G1 and G2 cell cycle arrest thereby reducing proliferation and cellular senescence. Inhibition of p21 expression is reported to increase the rate of the wound healing process [36-40]. Increased fibroblast cell survival and proliferation via activation of the PI3K–Akt–NF- $\kappa$ B pathway is probably mediated by interfering with the PCNA–p21 complex interaction [36].

### **Diabetic Foot Ulcers**

In diabetic foot ulcers, due to the hypoxic condition and inflammation, there is increased production of Reactive Oxygen Species (ROS) that results in upregulated levels of Metalloproteinase-9 (MMP-9), leading to tissue damage and poor wound healing [41]. When MMP-9 is expressed at excessive levels, it prevents the reestablishment of the dermal/epidermal junction and thereby limits epithelial migration and wound closure [42,43]. This is in contrast to the normal wound healing process, where transient MMP-9 expression may facilitate keratinocyte detachment and migration into the wound bed. Increased MMP-9 expression in chronic wound can cause keratinocytes to migrate into the wound, but they are unable to re-anchor themselves to the matrix [44,45,46]. Ongoing release of TNF- $\alpha$  provides a proximate mechanism for excess and continued MMP-9 production in chronic wounds [41].

Notch1 ICD expression in diabetic wounds is known to be significantly increased in the case of diabetic foot ulcers [47,48]. Notch1 inactivation in keratinocytes is sufficient to cancel the repressive effects of the Dll4–Notch1 loop on wound healing in diabetics, making Notch1 signalling an attractive local therapeutic target for the treatment of Diabetic foot ulcers (DFUs) [48,49,50].

Screening of potential drug targets identified from the wound healing signalling pathways will help us to identify novel compounds that can potentiate healing mechanisms [51,52].

Hordenine (4-[2-(Dimethylamino)ethyl] phenol) is a phenethylamine alkaloid that is naturally occurring in germinated barley (*Hordeum vulgare* L.). Hordenine has been demonstrated to be effectively inhibit hyperpigmentation [53,54] enhance mouse dermal-papilla cells (DPCs') activity, and accelerate hair regrowth [55]. So, hordenine was selected as a candidate to screen against the targets involved in the wound healing process. Further, biologically equivalent analogues of Hordenine were derived and docked with the wound healing targets.

## **Materials and Methods**

### **Software and Bioinformatics Tools used in the study**

#### **Wound healing bioinformatics tools**

Inhibition of selected targets like TYRP1, DCT,  $\beta$ 2-ARs, CK1, GSK3B, PCNA, MMP-9 and Notch1 ICD for potentiating wound healing were identified from literature and confirmed using the Laverne bioinformatics tool (<https://www.novusbio.com/pathways/wound-healing>).

#### **Protein and ligand retrieval**

The three-dimensional structures of selected targets were retrieved from the Protein Data Bank [56]. The 3D structures of the selected ligands were retrieved from the PubChem Compound database [57].

The pbdqt files were generated in Autodock1.5.7. Autodock 4.0 was run in Cygwin terminal. The results were compiled and the best poses were visualized in the Autodock tool 1.5.7 [58]. All graphical presentations of the docked complexes were illustrated using Discovery studio visualizer version v19.1.0.18287 (BIOVIA, San Diego, CA, USA) [59].

#### **Preparation of protein and ligand**

**Active binding site identification:** Structures of the protein and known inhibitor complexes of the target proteins were retrieved from Protein Data Bank (<https://www.rcsb.org>). Energy minimization of the coordinates of these ligands were performed using PRODRG server [60] selecting polar hydrogens only. The energy minimized ligands in pdb format were viewed in Visual Molecular Dynamics (VMD) [61]. VMD is a molecular visualization program for viewing established active binding sites. Residues that are exposed on the surface were identified using GETAREA 1.0, which provides solvent accessible surface area and its gradient for proteins [62].

## Molecular docking

Autodock 4.0 [58], was used for conduct molecular docking studies, and the top 10 conformations of the bound ligands were obtained in decreasing order.

The conformation with a root mean square deviation (RMSD) value of zero is considered to be the best [63, 64]. The ligand Hordenine was docked with the selected targets. Tyrosine related protein 1 (TYRP1) (PDB ID: 5M8L), Dopachrome tautomerase (DCT) (PDB ID: 1DPT),  $\beta$ 2 adrenergic receptors ( $\beta$ 2-ARs) (PDB ID:2R4R), Casein kinase 1 (CK1) (PDB ID:2IZS), Glycogen synthase kinase 3 beta (GSK3B) (PDB ID:3F88), Proliferating cell antigen (PCNA) (PDB ID:4D2G), Metalloproteinase-9 (MMP-9) (PDB ID:5TH6) and Notch1 I D receptor (PDB ID: 5FM8).

## Bioisosteric Replacement

Biologically equivalent replacements (bioisosteres) for Hordenine were obtained by replacing the hydroxyl and methyl functional groups using SwissBioisostere ([http:// www.swissbioisostere.ch](http://www.swissbioisostere.ch)) web-server interface [65]. Compounds having an improved biological performance in biochemical assays from the SwissBioisostere database were selected. The biological performance corresponds to 1,948 molecular targets and 30 target classes. The 2D structure of Hordenine was drawn using MarvinSketch 6.2 embedded in the SwissBioisostere server. Using the “Fragment 1” window in the SwissBioisostere, the 2 methyl groups and hydroxyl group were labeled as the -R groups and queried against the database. Biologically equivalent functional groups were detected based on matched molecular pair and mining bioactivity data in the ChEMBL database. A total of 166 equivalent replacements were identified by the webserver. The frequency of observations, activity difference distribution, success-based score, and chemical similarity between the fragments were also obtained. Six compounds that had better performance than Hordenine were shortlisted for further assessment.

## Pharmacokinetic Assessment (ADMET)

Predicting ADMET properties before subjecting the compound to resource intensive preclinical and clinical studies is very important to avoid failure of drug in later stages [66,67]. The ADMET properties of six compounds were computed using the web-based Swiss-ADME tool (<http://www.swissadme.ch/>) [68]. The ADME parameters, physicochemical descriptors,

pharmacokinetic properties, druglike nature and medicinal chemistry friendliness of the bioisosteres were obtained.

### **Molecular docking of Selected compounds**

To confirm the binding activity of the shortlisted bioisosteres to the protein targets, docking of bioisosteres that had nil-leadlikeness violations in above ADMET screening was performed with each of the target proteins using Autodock 4.0 and the docking results were visualized and illustrated using Discovery studio visualizer version v19.1.0.18287 (BIOVIA, San Diego, CA, USA)[59]. The protein-ligand complex interactions were visualized and assessed using protein–ligand interaction profiler (PLIP) at <https://plip-tool.biotec.tu-dresden.de>[69].

### **Molecular Dynamic (MD) simulations**

The molecule 5 (1-(5-amino-1H-1,2,4-triazol-3-yl)-N-[2-(4-chlorophenyl) ethyl]-N-methylpiperidin-4-amine) had high docking score for all the wound healing protein targets of wound healing selected in this study. This compound in complex with the CK1 receptor (-14.2 Kcal/mol) gave the lowest binding energy and thereafter subjected to MD simulations using the sander module of AMBER 14 software package [70] with the ff99 force field parameters. All simulations were done on CK1 (PDB ID 2IZS).

Crystal structures were downloaded from the RCSB protein data bank. Missing residues were modeled using Modeller version 9.11[71] with the sequences given in the PDB file. The Amber FF14SB force field was used for the proteins and Amber GAFF parameters were employed for the ligands. Hydrogen atoms of the ligands were modeled using the REDUCE program in Amber 14. The ligand atomic partial charges were then generated using the empirical charge model - AM1-BCC using the ANTECHAMBER program of Amber 14. Each complex was solvated in a TIP3P water box with a minimum distance of 8.0 from the surface of the complex to the edge of the simulation box. All runs were carried out for a time period of at least 30 nanoseconds. The simulation details are summarized in **Table 1**. A periodic truncated octahedron box was used for solvation of the protein in explicit TIP3P water molecules. The molecular systems were neutralized with Na<sup>+</sup> ions. The initial solvated structures were first subjected to 200 steps steepest descent energy minimization, whereas the solute atoms, including the protein, were restrained by a harmonic potential with a force constant of 100.0 kcal/mol/Å<sup>2</sup>. After the initial solvent minimization, the whole system was minimized using 200 steps of steepest descent minimization without harmonic restraints. The minimized structures were then subjected to an equilibration

protocol in which the temperature of the system was gradually raised from 100K to 300K over a 10ps period while holding both the volume and temperature constant, followed by another 10ps at 300K by holding the temperature and pressure constant while allowing the volume to change for adjusting solvent density. The initial velocities were randomly assigned from a maxwellian distribution at 100K. At the end of the equilibration, the average temperature of the final 5ps was 300K, and the average density was 1.0 g/ml. Long range electrostatic interactions were treated with the particle mesh Ewald method. Periodic boundary conditions were applied via both the nearest image and the discrete Fourier transform implemented as part of the particle mesh Ewald method. All bonds involving hydrogen atoms were restrained using the SHAKE algorithm with time steps of 2fs.. Global translation and rotation of the system (solvent and solute) was removed every 100 integration steps during the simulation. The initial 20ps stage was designed to equilibrate those particles that were added during the initial model-building process, including water molecules and hydrogen atoms, and to allow the systems to be solvated adequately. The initial 20ps trajectories were discarded. This was followed by the production stage in which both pressure (1.0 atm) and temperature (300K) were held constant by the Berendsen's coupling scheme.

**Table-1 The simulation details of (1-(5-amino-1H-1,2,4-triazol-3-yl)-N-[2-(4-chlorophenyl) ethyl]-N-methylpiperidin-4-amine) and Casein 1 kinase**

Simulation length (ns)	System Temp (K)	Total no of atoms	No of H <sub>2</sub> O molecules	Counter ions	Number of Counter ions added
30	300	53034	10872	Cl <sup>-</sup>	8

### MM-PBSA Calculation

The snapshots generated from MD simulations were used to post-process binding free energies by the single-trajectory MMPBSA method [72].

For a non-covalent binding reaction in the aqueous phase

$R + L \rightarrow R:L$ , where R, L, and R:L represent receptor, ligand, and complex, respectively.

The binding free energy,  $\Delta G_{\text{bind,aqu}}$ , can be computed as

$$\Delta G_{\text{bind,aqu}} = \Delta G_{\text{bind,vac}} + \Delta G_{\text{bind,solv}},$$

Where,  $\Delta G_{\text{bind,vac}}$  is the binding free energy in the vacuum phase, and  $\Delta G_{\text{bind,solv}}$  is the solvation free energy change upon binding

$$\Delta G_{\text{bind,solv}} = \Delta G_{\text{R:L,solv}} - \Delta G_{\text{R,solv}} - \Delta G_{\text{L,solv}},$$

Where,  $\Delta G_{\text{R:L,solv}}$ ,  $\Delta G_{\text{R,solv}}$  and  $\Delta G_{\text{L,solv}}$  are solvation free energies of complex, receptor and ligand, respectively.

Here the solvation free energies were computed by calculating two different components separately, polar and non-polar, both within the implicit solvation framework

$$\Delta G_{\text{solv}} = \Delta G_{\text{solv,polar}} + \Delta G_{\text{solv,nonpolar}}.$$

The polar part,  $\Delta G_{\text{solv,polar}}$ , can be calculated by solving the Poisson-Boltzmann (PB) equation. In cases where both the ionic strength and solvent potential are low, and when symmetric electrolytes are considered, the PB equation can be linearized to:

$$\nabla \cdot \epsilon \nabla \phi = -4\pi \rho_0 + \epsilon v \kappa^2 \phi,$$

where  $\kappa^2 = 8\pi e^2 I \epsilon v \kappa^2 / k_B T$ . Here  $v$  denotes the solvent,  $I$  represents the ionic strength of the solution, and is defined as  $I = \frac{1}{2} \sum c_i z_i^2$ . After solving potential  $\phi$ ,  $\Delta G_{\text{solv,polar}}$  can be computed as

$$\Delta G_{\text{solv,polar}} = \frac{1}{2} \sum q_i \phi_i.$$

The non-polar part,  $\Delta G_{\text{solv,non-polar}}$ , is typically estimated by the surface area (SA) method.

### **Absolute Binding Free Energy Calculation**

The standard free energy change,  $\Delta G_0$ , for binding can be expressed as

$$\Delta G_0 = -RT \ln Z_{\text{R:L}} / Z_{\text{R}} Z_{\text{L}} + RT \ln 8\pi^2 C_0.$$

Where,  $R$  is the gas constant,  $T$  is the temperature,  $C_0$  is the standard state concentration (1M).  $Z_{\text{R:L}}$ ,  $Z_{\text{R}}$ , and  $Z_{\text{L}}$  are the configuration integrals of the complex, receptor, and ligand, respectively. The configurational integrals are apparently very difficult to compute for typical proteins or protein complexes due to the extremely high dimensionalities of the integrals. In this study, it is approximated by the sum of the free energy change given the assumption of no configurational rearrangement and the free energy change upon configurational rearrangement,  $\Delta G_{\text{Conf}}$ . The free energy change without configurational rearrangement is approximated by the single-trajectory MMPBSA method,  $\Delta G_{\text{mmpbsa}}$ . The free energy change upon configurational rearrangement,  $\Delta G_{\text{Conf}}$ , is taken from a previous analysis. Therefore, the equation can be approximated as

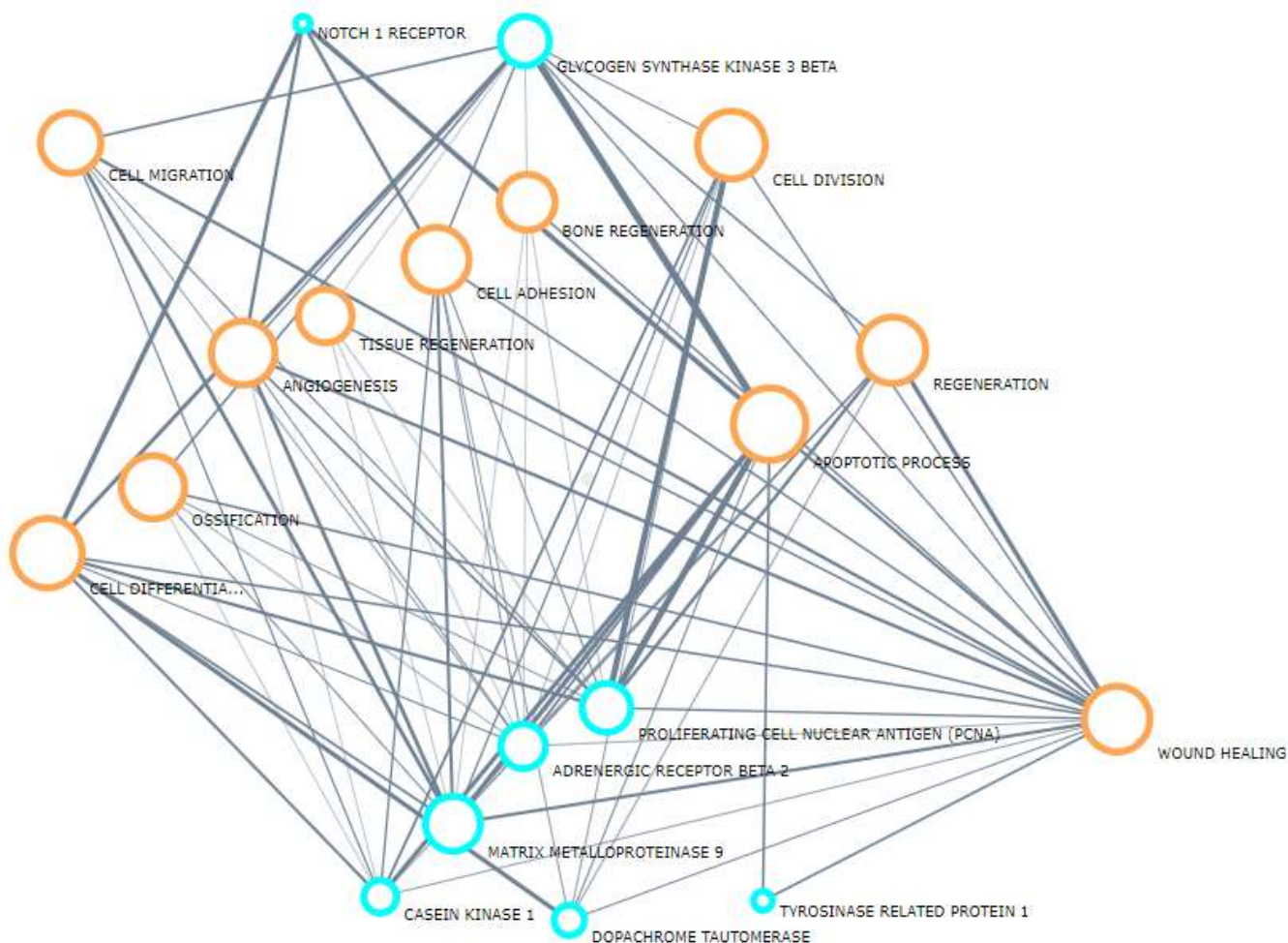
$$\Delta G_0 \sim \Delta G_{\text{mmpbsa}} + \Delta G_{\text{conf}} + RT \ln 8\pi^2 C_0.$$

Where,  $RT \ln 8\pi^2 C_0$  is a constant, with a value of 7.0 kcal/mol at the standard condition.

### **Results and discussion**

#### **Laverne Bioinformatics Tool**

The results obtained from the Laverne Bioinformatics tool is provided in the Fig.1.

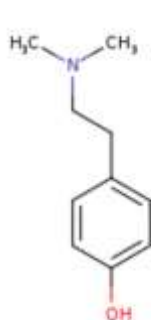


**Fig.1 Association of selected protein targets in wound healing mechanisms from Laverne Bioinformatics Tool. Blue circles indicate targets and the brown circles indicate association with the wound healing pathways.**

A network of proteins involved in the wound healing pathways was derived using the Laverne bioinformatics tool from Novus Biologicals. Hordenine, is found in a variety of plants and portrays several biological and pharmacological activities [73,74,75, 76]. As an alkaloid, hordenine is a promising candidate for the treatment of inflammatory diseases [77,78]. It promotes the healing of colonic ulcers by regulating the expression of tight junction proteins, including ZO-1 and occludin [76].

**Table 2: The inhibitory constant and binding energies of the selected wound healing targets**

Targets of wound healing	PDB ID	Binding Energy (kcal/mol)	Inhibitory constant	Ligand Efficiency (kcal/mol)
Tyrosine related protein 1 (TYRP1)	5M8L	-5.83	53.36 $\mu\text{m}$	-0.49
Dopachrome tautomerase (DCT)	1DPT	-4.66	385. 25 $\mu\text{m}$	-0.39
$\beta$ 2 adrenergic receptors ( $\beta$ 2-ARs)	2R4R	-5.19	157.58 $\mu\text{m}$	-0.43
Casein kinase 1 (CK1)	2IZS	-2.99	6.44mM	6.44
Glycogen synthase kinase 3 beta) GSK3B	3F88	-4.88	523.89 $\mu\text{m}$	-0.37
Proliferating cell antigen PCNA	4D2G	-6.23	27.04 $\mu\text{m}$	-0.52
Metalloproteinase-9 (MMP-9)	5TH6	-6.58	14.97 $\mu\text{m}$	-0.55
Notch1 I D receptor	5FM8	-5.42	106.9 $\mu\text{m}$	-0.45



**Hordenine**  
 $\text{C}_{10}\text{H}_{15}\text{NO}$   
 Pubchem ID CID68313

**Fig 2. Bioavailability radar of Hordenine**

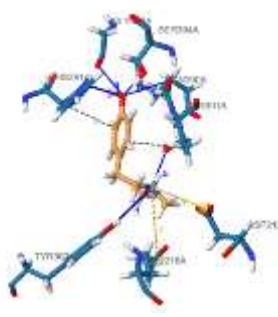
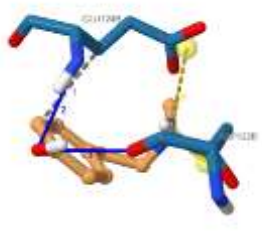
Table 2 presents the docking results of Hordenine. PCNA, MMP-9 and TYRP1 gave the lowest binding energy as compared to other protein targets. Hordenine had one lead likeliness violation with a synthetic accessibility score of 1 (Table 6).

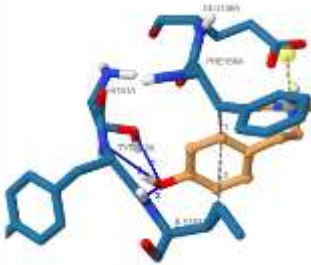
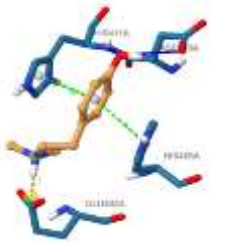
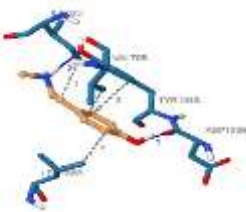
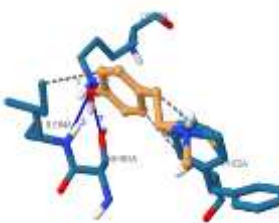
MMP-9 has been proven to be a prime candidate for disordered wound healing; reducing its levels in the wounds has been associated with resolution of the pathological condition [80]. A previous study showed that increased cell survival and repairing of fibroblast proliferation resulted in improved wound healing property via activation of the PI3K–Akt–NF- $\kappa$ B pathway which is mainly mediated by inhibition of the PCNA-p21 complex interaction [36]. Abnormal skin pigmentation is noticed after skin injuries such as burns, wound, or laser surgery, and during the wound healing response [84]. Though the binding energy of MMP-9 and PCNA are low, when


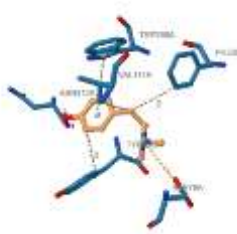
considering the molecular interactions of these targets, TYRP1 showed the maximum number of interactions with binding energy of -5.83 kcal/mol and an appreciably greater number of hydrogen bonds (Table 3). Inhibition of tyrosine metabolism play an important role in the initial stage of skin repair by targeting TYRP1 or DCT in keratinocytes [81,82]; they have been also proved to have a reducing property on the level of skin cell melanin pigmentation and skin whitening [53, 81].

As hordenine could not establish a binding energy beyond -7 kcal/mol for any of the targets, further biologically equivalent replacements (bioisosteres) for Hordenine were generated using SwissBioisostere version 2021(Fig 3). Around 166 Bioisosteres were generated of which 6 compounds that had improved biological activity were shortlisted (Table 6).

**Table 3 Interactions formed between Hordenine and the wound healing targets along with interacting residues and distance (Å)**

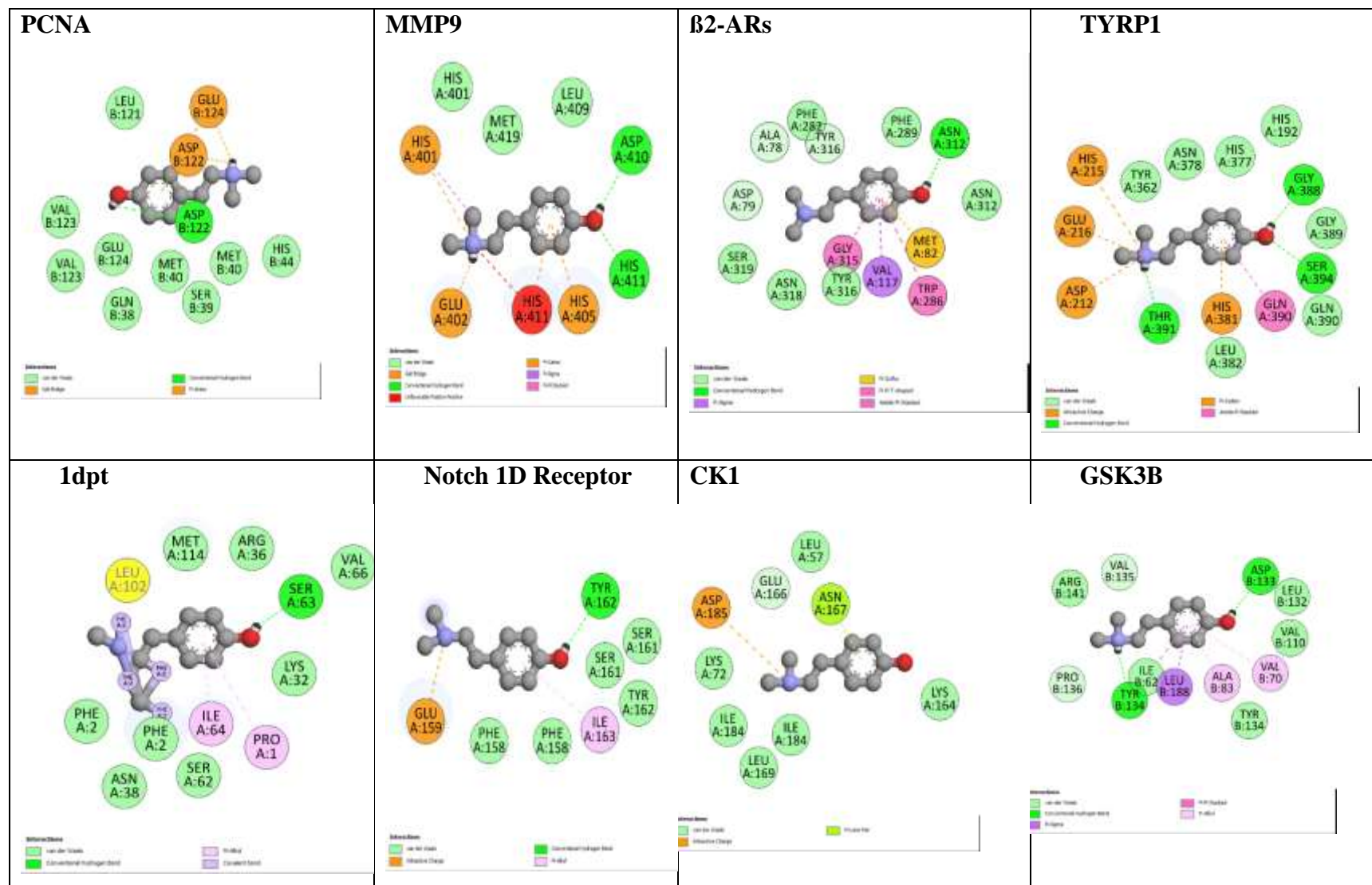
<b>Targets</b>	<b>Hydrophobic Interactions</b>	<b>Hydrogen Bonds</b>	<b>Salt Bridges</b>	<b><math>\pi</math>-Stacking Index</b>	<b>Interactions</b>
<b>TYRP1</b>	<b>2</b> 381HIS(3.99) 391THR (3.93)	<b>6</b> 362TYR(3.21) 381HIS(2.59) 388GLY(2.01) 390GLN(2.79) 391THR(2.07) 394SER(2.58)	<b>2</b> 212ASP (4.99) 216GLU (5.05)		
<b>PCNA</b>	<b>1</b> 124GLU (3.19)	<b>2</b> 122ASP (2.19) 124GLU(2.13)	<b>2</b> 122ASP (3.4) 12BGLU (3.83)		

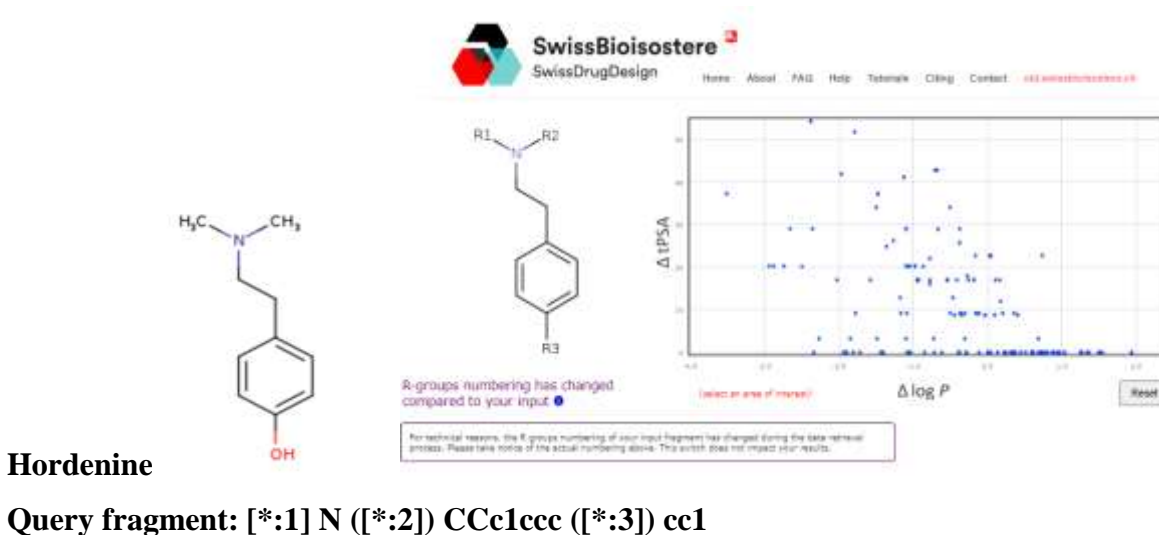
<b>Notch1 D</b>	<b>2</b> 158PHE (2.98) 163ILE(3.47)	<b>3</b> 161SER(2.03) 162TYR(3.27) 162TYR(2.23)	<b>1</b> 159GLU (2.7)		
<b>MMP9</b>		<b>2</b> 410AASP (2.21) 411AHIS (2.05)	<b>1</b> 402AGL U (2.46)	<b>2</b> 405AHIS (3.54) 411AHIS (3.87)	
<b>GSK3B</b>	<b>4</b> 62ILE(3.2) 70VAL(3.53) 134TYR (3.72) 188LEU(3.46)	<b>2</b> 133BASP (1.88) 134BTYR (2.16)			
<b>DPT1</b>	<b>3</b> 2PHE(2.54) 2PHE(3.11) 64ILE(3.58)	<b>3</b> 32LYS(2.09) 63SER(1.77) 64ILE(1.85)			

<b>ck1</b>	<b>2</b> 166GLU (2.91) 185ASP (3.75)	<b>1</b> 164LYS (2.11)	<b>1</b> 185ASP (5.06)		
<b>β2-ARs</b>	<b>3</b> 117VAL (3.23) 282PHE (3.77) 316TYR (3.38)	<b>1</b> 312ASN (2.07)	<b>1</b> 79AASP (4.73)	<b>1</b> 286TRP (4.68)	

■ Protein  
 ■ Ligand  
 ● Water  
 ● Charge Center  
 ○ Aromatic Ring Center  
 ● Metal Ion  
 .... Hydrophobic Interaction  
— Hydrogen Bond  
 ....  $\pi$ -Stacking (perpendicular)  
 .... Salt Bridge  
 ....  $\pi$ -Stacking (parallel)  
 — Halogen bond

**Fig 3** Intermolecular interactions between Hordenine against wound healing targets





**Fig 4: Query fragment for SwissBioisostere**

The query fragment for Hordenine was provided as input fragment as indicated: [\*:1] N ([\*:2]) CCc1ccc ([\*:3]) cc1 (Fig. 4)

The main objective of a bioisosteric replacement is creating a new molecule with similar biological properties as that of the parent compound; such modifications have been used to improve activity in several studies [83,84,85,86,87,88].

The pharmacological and physicochemical properties predicted by Swiss-ADME website are summarized in Table 6. The physicochemical properties of the compounds show that all 6 compounds had molecular weight less than 500 g/mol which is an important parameter for a small molecule to possess drug likeliness property [90]. The topological polar surface area (TPSA) is established as a good indicator of drug absorption in the intestine (TPSA less than 140 Å<sup>2</sup>) and for penetration of the blood-brain barrier (TPSA less than 60 Å<sup>2</sup>) [89,91, 92]. In this study all the compounds had a TPSA value of 74.07 Å<sup>2</sup>, indicating that all the 6 molecules had high GI absorption but did not possess adequate blood brain permeability [93]. The partition coefficient between n-octanol and water (log Po/w) is the classical descriptor for lipophilicity, which was assessed and collectively reported (consensus log Po/w) by the predictive models in SWISS - ADME; i.e. iLOGP, XLOGP3, WLOGP, MLOGP, and SILICOS-IT [69]. Log P VALUE should be  $\leq 5$  [94, 95]. The number of rotatable bonds (NRB) is another indication of the flexibility of a

compound [96, 97, 98]. The molecules tested in this study had rotatable bonds ranging from 5-7. A drug candidate is predicted to be orally non-bioavailable when its rotatable bonds are more than 9 [69,96,98,99].

Thus molecules 3,4 and 5 may be effluxed out from the GIT or Brain as it is a substrate for P-gp. Based on whether these molecules could serve as substrates of the permeability glycoprotein (Pgp) provides information about its active efflux nature through several biological membranes like the gastrointestinal wall or the brain [100,101]. It jeopardizes the success of drug delivery; however, strategies are being developed to overcome P-gp mediated drug transport [102]. Modifying the action of the P-gp through inducers, inhibitors or genetic polymorphisms are being tried[103], Employing natural inhibitors like curcumin [104], Piperine [105], Capsaicin [106], 15[6] Gingerol [107], Limonin [108] is found to be a much safer and more economical option.

Predicting the tendency of the molecule to inhibit cytochromes P450, plays an important role in determining the biotransformation of these molecules [109, 110, 111]. These compounds may variably interact with any cytochrome P450 isoforms as shown in Table 6, indicating that isoforms may be involved in the biotransformation of the molecule by inhibiting some of the cytochrome P450 isoforms. The bioavailability score of all six molecules was 0.55 without violating any of the filters employed for drug likeliness in SWISS-ADME [112, 113, 114].

The Bioavailability Radar plot provides quick information on the drug-likeness of a molecule of interest. Six physicochemical properties are taken in to account: LIPO (Lipophilicity XLOGP3 between 0.7 and + 5.0), SIZE (MW between 150 and 500 g/mol), POLAR (Polarity TPSA between 20 and 130 Å<sup>2</sup>), INSOLU (Insolubility log S not higher than 6), INSATU (Insaturation : fraction of carbons in the sp<sup>3</sup> hybridization not less than 0.25) and FLEX (Flexibility no more than 9 rotatable bonds) [69]. The bioavailability radar for all the molecules are provided in Table 7. The pink area exemplifies the optimum physicochemical space for each property predicted to be orally bioavailable [95].

As shown by several authors synthetic accessibility when scaled between 1 and 10, molecules with the high synthetic accessibility score (SA score) are difficult to synthesize, whereas, molecules with low SA scores are easily synthetically accessible [115, 116].

The human skin penetrating ability is demonstrated by the human skin permeability coefficient (Logkp) [119] of Hordenine (−5.83 cm/s). The molecule 5(−6.02 cm/s) has a high permeability coefficient suggesting that it would be a good candidate for an external wound healing medication [117].

In case of humans CYP3A4, is the most abundantly expressed Cytochrome P450 enzyme that metabolizes 30% to 50% of the marketed drugs [121]. In this study both hordenine and molecule 5 are non-inhibitor of CYP 3A4 indicating that drug-drug interactions will be very low or absent with no side effects [118, 119, 120].

Overall, the pharmacokinetic assessment (ADMET) showed that molecule 5 had nil leadlikeness violations and Hordenine had one violation, and had better SA scores of 2.6 and 1, respectively as compared to the other compounds. Based on the above features, since molecule 5 satisfies all Lipinski rules and has a wider safety profile, this was selected for further docking studies using Autodock 4.0 against the wound healing targets.

**Table 4 : Molecular docking results of compound (1-(5-amino-1H-1,2,4-triazol-3-yl)-N-[2-(4-chlorophenyl) ethyl]-N-methylpiperidin-4-amine)**

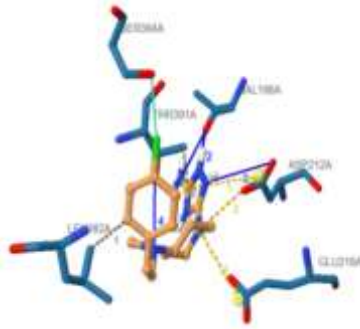
Bioisosteres (Molecule 5)	β2-ARs	TYRP1	PCNA	Notch 1	GSK3B	CK1	1DPT	MMP9
<b>CHEMBL4065553</b>	<b>Binding Affinity (Kcal/mol)</b>							
<b>Binding energy (Kcal/mol)</b>	-8.19	-9.44	-9.89	-7.44	-5.7	-14.41	-6.4	-11.72
<b>Ligand efficiency (kcal/mol)</b>	-0.36	-0.41	-0.43	-0.32	-0.25	-0.63	-0.28	-0.51
<b>Inhibitory constant</b>	1.02uM	119.76nM	56.49nM	3.52uM	66.59uM	27.18pM	20.26uM	2.56nM

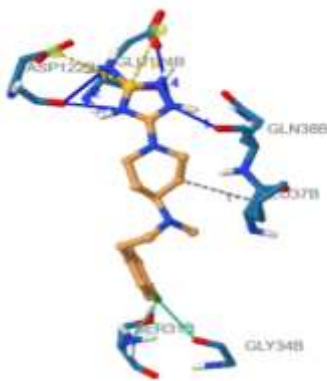
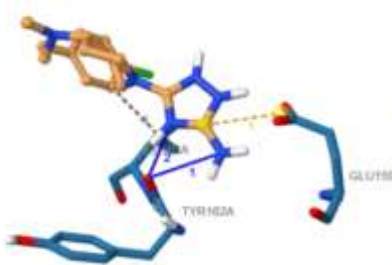
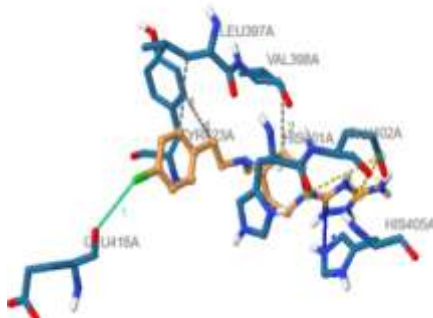
The lowest binding affinity refers to the most stable binding between the protein and its ligands. The binding energy results calculated by Autodock 4.0 are presented in Table 4. The molecule 5 had good molecular interactions with all the wound healing targets including hydrophobic

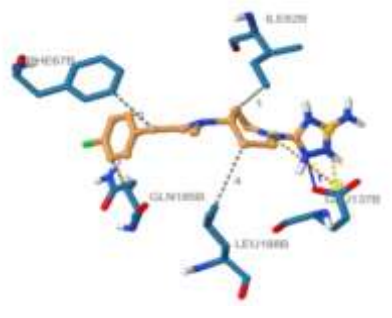
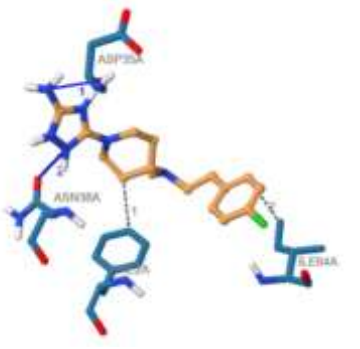
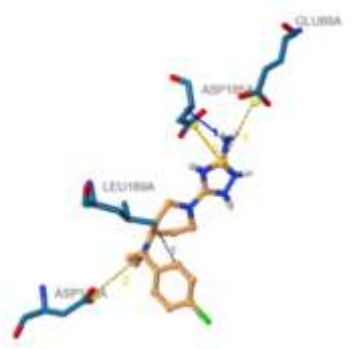
Interactions, Hydrogen Bonds, Halogen Bonds and Salt Bridges. The docked structures were further studied using Discovery studio 4.5 Visualizer and the images are presented in Fig.7 [121,122,123], and PLIP server (Table 5) [124,125].

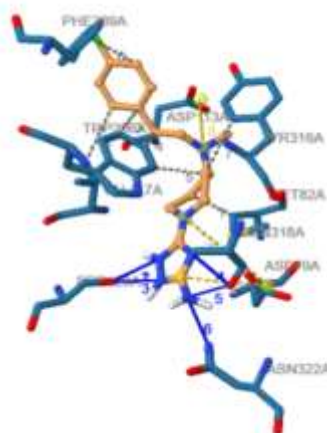
As hydrogen bonds play a major role in the stabilization of protein-ligand complexes [126], the interactions formed between Molecule 5 and wound healing targets from this study varied from 1-7, with other interactions including hydrophobic interactions, halogen bonds and salt bridges, which all indicate that the interaction formed is highly stable [127].

The molecule 5 demonstrated lowest binding affinity with most of the wound healing targets, ranging from -5.7 to -14.41 Kcal/mol. As molecule 5 had lowest binding affinity of -14.41 Kcal/mol against CK1 with ligand efficiency of -0.63 Kcal/mol and inhibitory constant of 27.18pM it is further subjected to molecular dynamic simulations. The known inhibitor of CK1, Suinitinib [128,129] had a binding affinity of -8.1Kcal/mol, compared to which molecule 5 had a lowest binding affinity. **Table 5 Interactions between Molecule 5 and wound healing Targets along with interacting residues and distance (Å)**

Targets	Hydrophobic Interactions	Hydrogen Bonds	Halogen Bonds	Salt Bridges	Interactions
<b>TYRP1</b>	<b>2</b> 382LEU(3.6) 391THR (3.74)	<b>4</b> 196VAL (2.14) 196VAL (1.93) 212ASP (3.42) 391THR (2.78)	<b>1</b> 394SER (2.92)	<b>3</b> 212ASP (4.96) 212ASP ( 4.29) 216GLU (4.07)	

<b>PCNA</b>	<b>1</b> 37LEU (3.84)	<b>4</b> 38GLN (1.92) 122ASP (2.25) 122ASP (2.12) 124GLU (3.05)	<b>2</b> 31SER (3.3) 34GLY (3.32)	<b>2</b> 122ASP (4.2) 124GLU (4.1)	
<b>Notch 1D</b>	<b>1</b> 163ILE(3.39)	<b>2</b> 162TYR (3.57) 162TYR (2.71)	<b>1</b> 159GLU (3.2)	<b>Nil</b>	
<b>MMP9</b>	<b>4</b> 397LEU(3.93) 398VAL(3.4) 401HIS(3.84) 423TYR(3.64)	<b>1</b> 405HIS (3.42)	<b>1</b> 416GLU (3.83)	<b>2</b> 402GLU (4.63) 402GLU (2.86)	

<b>GSK3B</b>	<b>4</b> 62ILE(3.93) 67PHE(3.22) 185GLN(3.32) 188LEU(4)	<b>1</b> 137GLU (2.18)	<b>Nil</b>	<b>2</b> 137GLU (3.67) 137GLU (5.3)	
<b>DPT1</b>	<b>2</b> 2PHE (3.39) 64ILE(3.75)	<b>2</b> 35ASP (2.08) 38ASN (2.17)	<b>Nil</b>	<b>Nil</b>	
<b>CK1</b>	<b>1</b> 169LEU (3.76)	<b>1</b> 185ASP (3.09)	<b>Nil</b>	<b>3</b> 86GLU (4.47) 125ASP (4.68) 185ASP (4.02)	

β2-ARs	7	6	Nil	3	
	82AMET(3.12)	120ASER		79AASP	
	117AVAL(3.37)	(1.86)		(5.38)	
	286ATRP(4)	120ASER		79AASP	
	286ATRP(3.65)	(2.21)		(4.24)	
	286ATRP(3.13)	120ASER		3AASP(4.6)	
	289APHE(3.87)	(2.32)			
	316ATYR(3.32)	318AASN			
		(3.06)			
		318AASN			
		(2.24)			
		322AASN			
		(2.46)			



**Table 6 Pharmacokinetic Assessment (ADMET)**

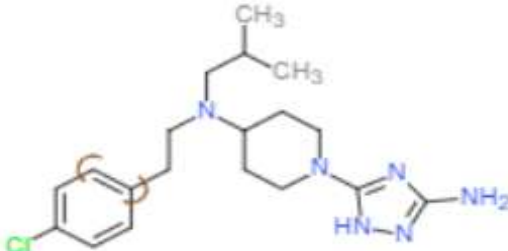
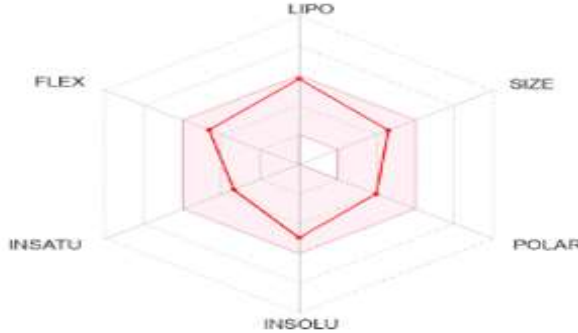
	Molecule	1	2	3	4	5	6	H*
PhysicoChemical properties	<b>Molecular Weight(g/mol)</b>	376.93	362.9	379.3	393.32	334.85	348.87	165.23
	<b>#Heavy atoms</b>	26	25	23	24	23	24	12
	<b>#Aromatic heavy atoms</b>	11	11	11	11	11	11	6
	<b>Fraction Csp3</b>	0.58	0.56	0.5	0.53	0.5	0.53	0.4
	<b>#Rotatable bonds</b>	7	6	5	6	5	6	3
	<b>#H-bond acceptors</b>	3	3	3	3	3	3	2

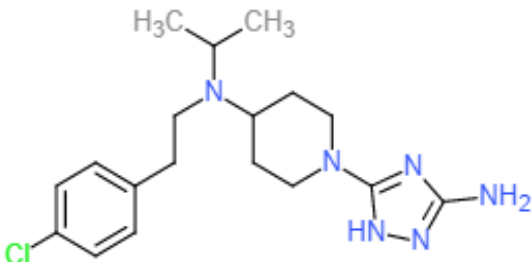
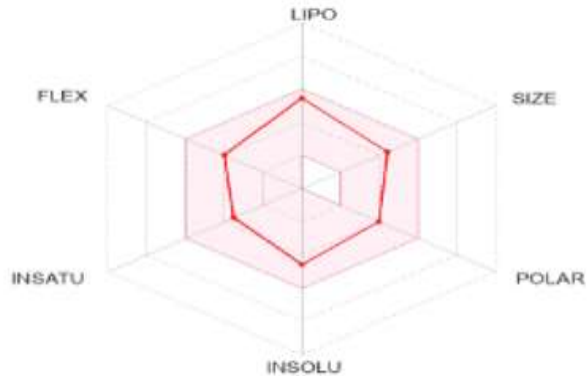
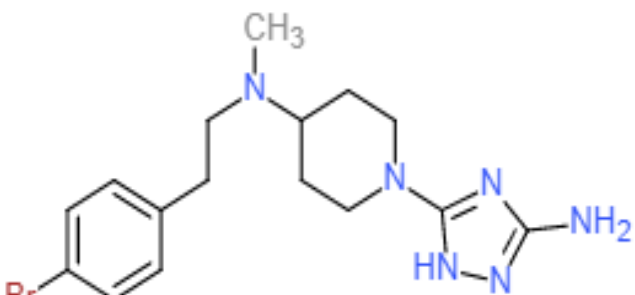
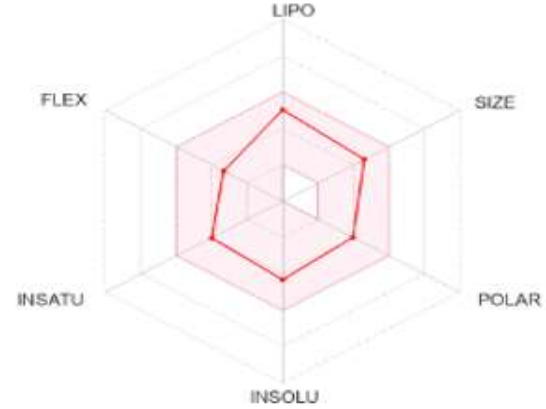
	<b>#H-bond donors</b>	2	2	2	2	2	2	1
	<b>MR</b>	111.47	106.66	99.74	104.55	97.05	101.86	50.75
	<b>TPSA</b>	74.07	74.07	74.07	74.07	74.07	74.07	23.47
<b>Lipophilicity</b>	<b>iLOGP</b>	2.98	2.64	2.37	2.46	2.31	2.31	2.11
	<b>XLOGP3</b>	4.6	4.07	3.33	3.7	3.27	3.64	2.08
	<b>WLOGP</b>	2.84	2.59	1.92	2.31	1.81	2.2	1.5
	<b>MLOGP</b>	2.97	2.74	2.39	2.63	2.27	2.51	1.83
	<b>Silicos-IT Log P</b>	2.83	2.44	1.89	2.27	1.85	2.23	1.59
	<b>Consensus Log P</b>	3.24	2.9	2.38	2.67	2.3	2.58	1.82
<b>Pharmacokinetics</b>	<b>GI absorption</b>	High	High	High	High	High	High	High
	<b>BBB permeant</b>	Yes	Yes	Yes	Yes	Yes	Yes	Yes
	<b>Pgp substrate</b>	No	No	Yes	No	Yes	Yes	No
	<b>CYP1A2 inhibitor</b>	No	No	Yes	No	No	No	Yes
	<b>CYP2C19 inhibitor</b>	Yes	Yes	Yes	Yes	No	Yes	No
	<b>CYP2C9 inhibitor</b>	No	No	No	No	No	No	No
	<b>CYP2D6 inhibitor</b>	No	No	Yes	No	Yes	No	No
	<b>CYP3A4 inhibitor</b>	Yes	Yes	Yes	Yes	No	Yes	No
	<b>log Kp (cm/s)</b>	-5.33	-5.62	-6.25	-6.07	-6.02	-5.84	-5.83
<b>Drug</b>	<b>Lipinski #violations</b>	0	0	0	0	0	0	0

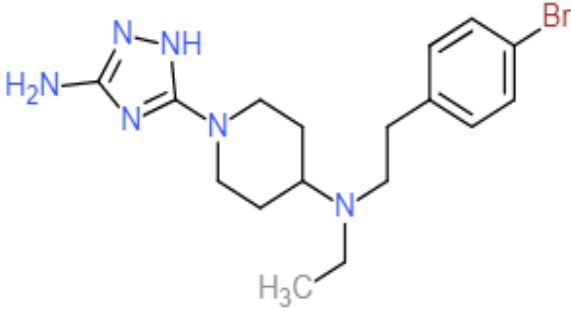
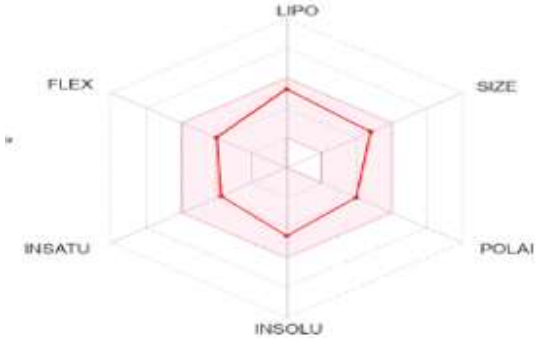
<b>Ghose #violations</b>	0	0	0	0	0	0	0
<b>Veber #violations</b>	0	0	0	0	0	0	0
<b>Egan #violations</b>	0	0	0	0	0	0	0
<b>Muegge #violations</b>	0	0	0	0	0	0	1
<b>Bioavailability Score</b>	0.55	0.55	0.55	0.55	0.55	0.55	0.55
<b>PAINS &amp; Brenk #alerts</b>	0	0	0	0	0	0	0
<b>Leadlikeness #violations</b>	2	2	1	2	0	1	1
<b>Synthetic Accessibility</b>	2.94	2.82	2.65	2.76	2.6	2.71	1

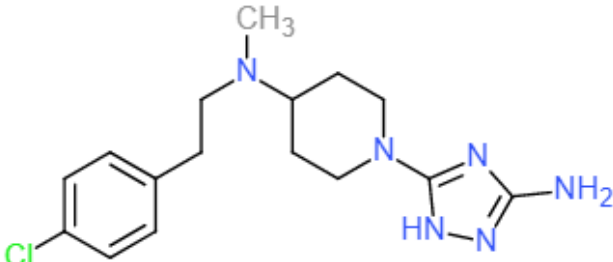

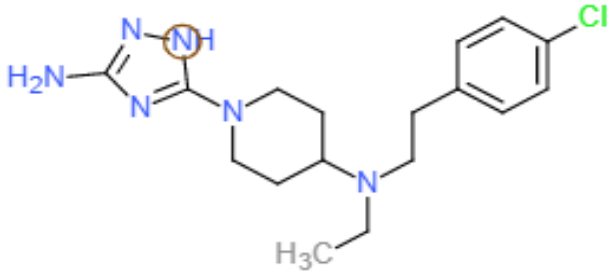
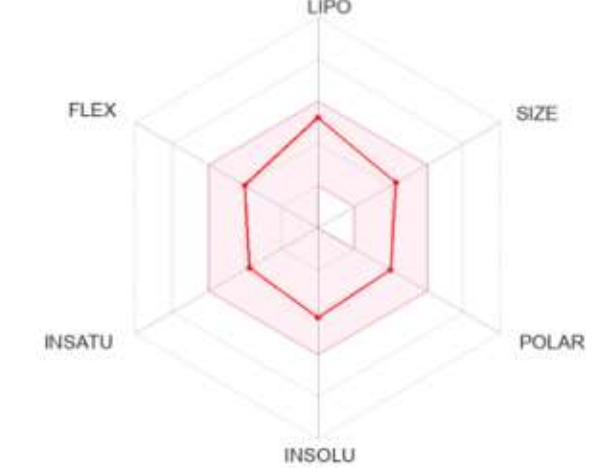
\*H Hordenine

**Table 7**ADMET properties and Bioavailability Radar Schematic diagram of Bioavailability Radar for Drug likeness of molecule

Sl.No.	Molecule	Structure	Bioavailability Radar
1	Molecule 1 ChEMBL4076989 C <sub>19</sub> H <sub>29</sub> ClN <sub>6</sub> PubchemCID: 118165440 1-(5-amino-1 <i>H</i> -1,2,4-triazol-3-yl)- <i>N</i> -[2-(4-chlorophenyl) ethyl]- <i>N</i> -(2-methylpropyl)piperidin-4-amine		

2	<p>Molecule 2</p> <p>CHEMBL4075848</p> <p>C<sub>18</sub>H<sub>27</sub>CIN<sub>6</sub></p> <p>PubchemCID:118165621</p> <p>1-(5-amino-1H-1,2,4-triazol-3-yl)-N-[2-(4-chlorophenyl) ethyl]-N-propan-2-ylpiperidin-4-amine</p>		
3	<p>Molecule 3</p> <p>CHEMBL4086986</p> <p>C<sub>16</sub>H<sub>23</sub>BrN<sub>6</sub></p> <p>PubchemCID:118165313</p> <p>1-(3-azanyl-1~{H}-1,2,4-triazol-5-yl)-~{N}-[2-(4-bromophenyl) ethyl]-~{N}-methyl-piperidin-4-amine</p>		

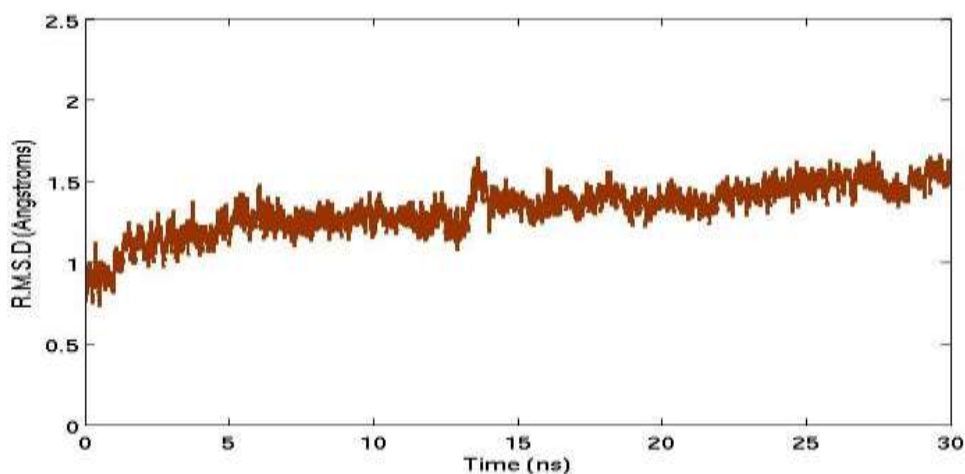
4	<p>Molecule 4</p> <p>CHEMBL4098997</p> <p>C<sub>17</sub>H<sub>25</sub>BrN<sub>6</sub></p> <p>PubchemCID:118165200</p> <p>1-(5-amino-1H-1,2,4-triazol-3-yl)-N-[2-(4-bromophenyl) ethyl]-N-ethylpiperidin-4-amine</p>		

<p>5</p>	<p>Molecule 5            CHEMBL4065553            C<sub>16</sub>H<sub>23</sub>ClN<sub>6</sub>            PubchemCID:118165354  <b>1-(5-amino-1H-1,2,4-triazol-3-yl)-N-[2-(4-chlorophenyl)ethyl]-N-methylpiperidin-4-amine</b></p>		
<p>6</p>	<p>Molecule 6            CHEMBL4072036            C<sub>17</sub>H<sub>25</sub>ClN<sub>6</sub>            PubchemCID:118165257  <b>1-(5-amino-1H-1,2,4-triazol-3-yl)-N-[2-(4-chlorophenyl) ethyl]-N-ethylpiperidin-4-amine</b></p>		

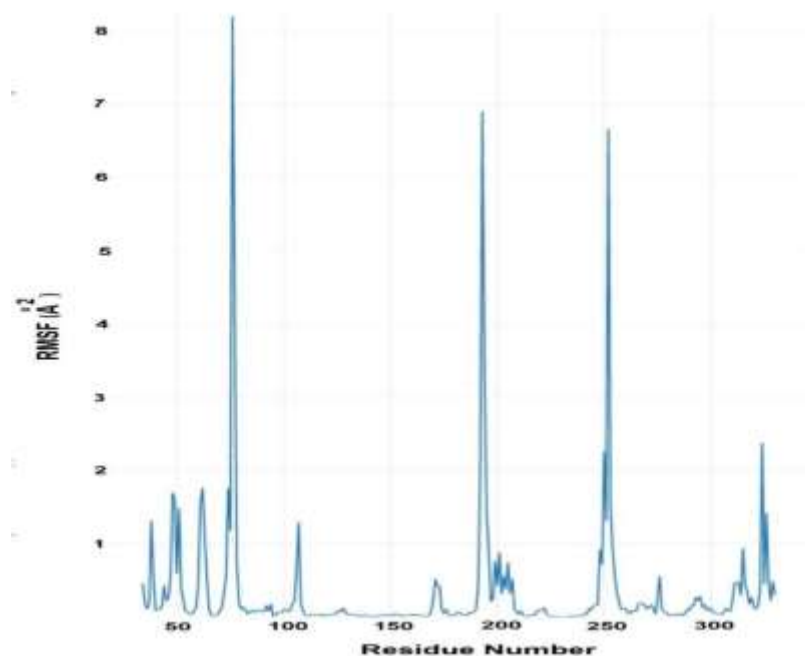


### Stability of the MD simulations

Root Mean Square Deviation (RMSD) of the 30ns MD simulation carried out in aqueous medium. The trajectories of RMSDs with respect to the minimized starting structure are shown in **Fig. 5**.



**Figure 5: RMSD calculated for 30ns MD simulation of Casein 1Kinase**

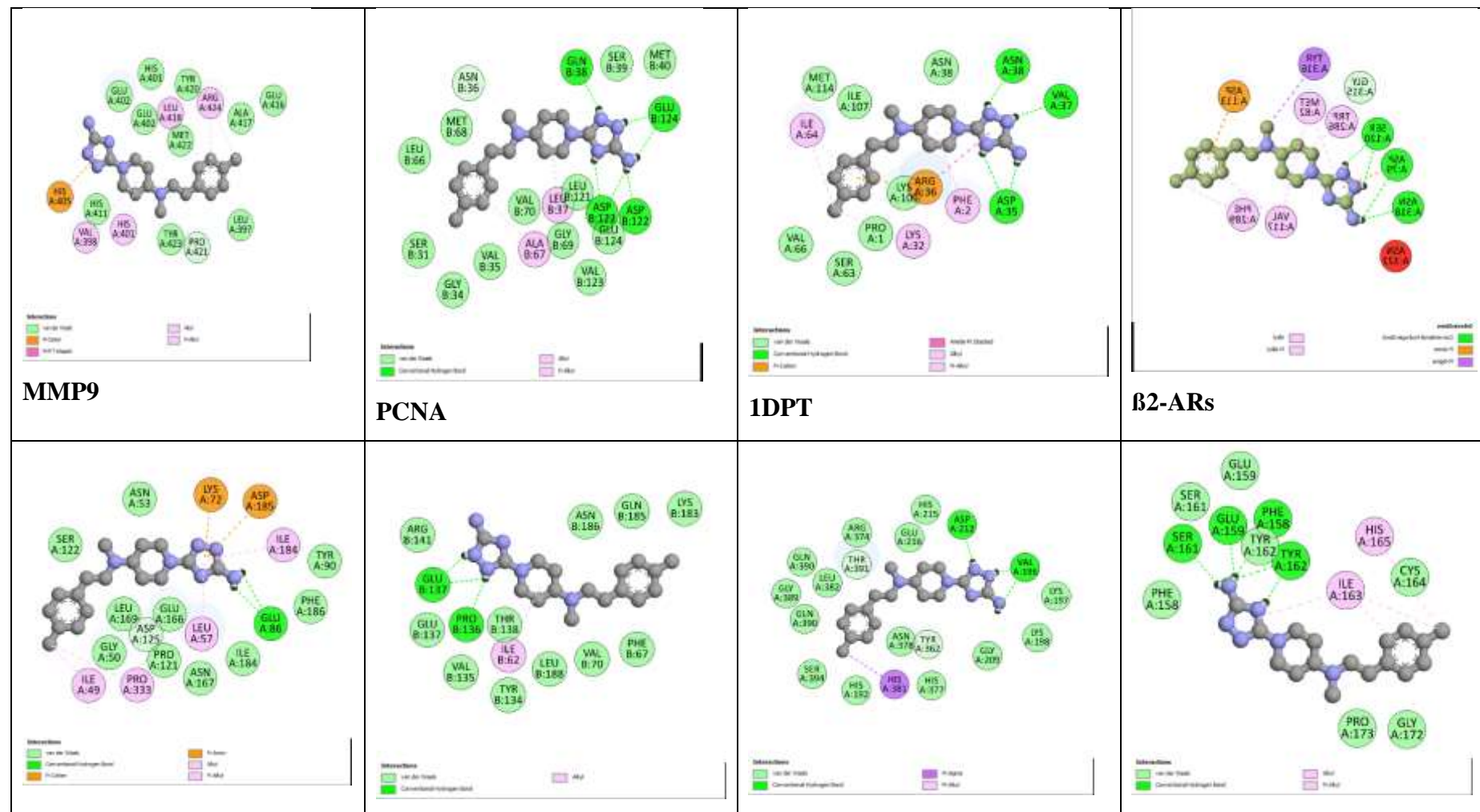


**Figure 6: Root Mean Square Fluctuations (RMSF)**

The C $\alpha$  RMSD values were found to be within 1.6 Å throughout the simulation for the system. This shows that the protein-ligand complex did not undergo any major conformational change and was stable throughout the simulation. Root Mean Square Fluctuations (RMSF) is a calculation of individual residue flexibility, i.e., how much a particular residue moves (fluctuates) during a simulation. Loop residues involved in ligand binding (Residues 49 to 57) show minimal fluctuations as compared to other loop residues (Residues 75 -81, 192-217, 245 -255). This corroborates with the good binding score obtained in docking and MMPBSA calculations.

The binding free energy was estimated to be -10.44 Kcal / mol from MMPBSA calculations. This confirms that the ligand 1-(5-amino-1H-1,2,4-triazol-3-yl)-N-[2-(4-chlorophenyl) ethyl]-N-methylpiperidin-4-amine has good binding interaction with the active site loop of Casein 1 Kinase giving strong evidence that this molecule could be a promising candidate for wound healing.

**Fig 7 Intermolecular interactions between 1-(5-amino-1H-1,2,4-triazol-3-yl)-N-[2-(4-chlorophenyl)ethyl]-N-methylpiperidin-4-amine and wound healing targets**



CK1	GSK3B	TYRP1	Notch 1D Receptor

## Conclusion

The insilico analysis predicted that, the primary molecule Hordenine and the bioisostere **1**-(5-amino-1H-1,2,4-triazol-3-yl)-N-[2-(4-chlorophenyl) ethyl]-N- ethylpiperidin-4-amine can be used in combination for both acute and chronic wounds. The CK1-bioisostere ligand complex did not undergo any major conformational change and was stable throughout the simulation confirming that the compound can be a promising drug candidate. This compound is also effective for Diabetic wound healing with maximum hydrogen bond interactions against Notch 1D receptor. They can be employed further in in- vivo cell culture assays and animal wound healing models for further confirmatory studies.

## Declaration of competing interest

The authors declare that they have no known competing financial interests or personal relationships that could have appeared to influence the work reported in this paper.

## Acknowledgments

Authors are thankful to the Vels Institute of Science, Technology and Advanced Studies (VISTAS) for infrastructure and facilities.

## Funding Source

This study does not receive any funding.

## References

1. G.C.Gurtner,S.Werner,Y.Barrandon, M.T.Longaker, Wound Repair and Regeneration, Nature 453 (2008) 314-321.
2. S.A.Eming,P.Martin,M.Tomic-Canic, Wound repair and regeneration: mechanisms, signaling, and translation. Sci. Transl. Med. 6(265) (2014) 265sr6. doi: 10.1126/scitranslmed.3009337
3. R.A.F.Clark, Overview and General Considerations of Wound Repair. In: Clark, R.A.F. Henson, P.M. (eds) The Molecular and Cellular Biology of Wound Repair. Springer, Boston, MA(1998).[https://doi.org/10.1007/978-1-4615-1795-5\\_1](https://doi.org/10.1007/978-1-4615-1795-5_1)
4. S.Guo, L.A.Dipietro, Factors affecting wound healing. J. Dent. Res. 89(3) (2010) 219-29. doi: 10.1177/0022034509359125.

5. F.M.Thiruvoth, D.P. Mohapatra, D.Kumar, S.R.K.Chittoria, V.Nandhagopal. Current concepts in the physiology of adult wound healing. *Plast. Aesthet. Res.* 2 (2015) 250-6. <http://dx.doi.org/10.4103/2347-9264.158851>
6. M.Rodrigues, N.Kosaric, C.A. Bonham, G.C.Gurtner, Wound healing: A Cellular Perspective, *Physiol. Rev.* 99 (2019) 665–706 doi:10.1152/physrev.00067.20176650031-9333/19
7. R.G.Frykberg , J.Banks, Challenges in the Treatment of Chronic Wounds. *Adv. Wound Care (New Rochelle).* 4(9) (2015) 560-582. doi: 10.1089/wound.2015.0635.
8. G.S.Schultz, G.A.Chin, L. Moldawer, R.F. Diegelmann, Principles of Wound Healing. In: R.Fitridge ,M. Thompson , editors. *Mechanisms of Vascular Disease: A Reference Book for Vascular Specialists* [Internet]. Adelaide (AU): University of Adelaide Press; (2011). 23. Available from: <https://www.ncbi.nlm.nih.gov/books/NBK534261/>
9. H.J. Zhu, M.Fan, W.Gao, *Identification of potential hub genes associated with skin wound healing based on time course bioinformatic analyses. BMC Surg.* 21 303 (2021). <https://doi.org/10.1186/s12893-021-01298-w>
10. S.C.Daubner , T.Le , S.Wang . Tyrosine hydroxylase and regulation of dopamine synthesis. *Arch. Biochem. Biophys.* 508(1) (2011) 1-12. doi: 10.1016/j.abb.(2010).12.017.
11. Y. Xu , AH. Stokes , R. Jr. Roskoski , K.E. Vrana, Dopamine, in the presence of tyrosinase, covalently modifies and inactivates tyrosine hydroxylase. *J. Neurosci. Res.* 54(5) (1998) 691-7. doi:10.1002/(SICI)1097-4547(19981201)54:5<691::AID-JNR14>3.0.CO;2-F.
12. Y.F. Fan, S. Zhu,X. Hou, F.B. Zhao, D.F. Pan, Q.S. Xiang, Y.W. Qian, X.K. Ge, G.B. Wang, P, Spectrophotometric Assays for Sensing Tyrosinase Activity and Their Applications. *Biosensors 11* (2021) 290. <https://doi.org/10.3390/bios11080290>
13. A. Tingaud-Sequeira, E. Mercier, V. Michaud, B. Pinson, I. Gazova, E. Gontier, F.Decoeur, L. McKie, I.J. Jackson, B. Arveiler, S. Javerzat, The *Dct*<sup>-/-</sup> Mouse Model to Unravel Retinogenesis Misregulation in Patients with Albinism. *Genes (Basel).* 13(7) (2022) 1164. doi: 10.3390/genes13071164.

14. C.E.Pullar, A. Rizzo, R.R.Isseroff, Beta-Adrenergic receptor antagonists accelerate skin wound healing: evidence for a catecholamine synthesis network in the epidermis. J. Biol. Chem. 281(30) (2006) 21225-21235. doi: 10.1074/jbc.M601007200.
15. R.K.Sivamani, S.T. Lam, R.R. Isseroff. Beta adrenergic receptors in keratinocytes. Dermatol. Clin. 25(4) (2007) 643-53, x. doi: 10.1016/j.det.2007.06.012.
16. H.Y. Yang, P.Steenhuis, A.M. Glucksman, Z. Gurenko, T.D. La, R.R. Isseroff, Alpha and beta adrenergic receptors modulate keratinocyte migration. PLoS ONE 16(7) (2021) e0253139. <https://doi.org/10.1371/journal.pone.0253139>
17. I.Pastar, O.Stojadinovic, N.C Yin, H. Ramirez, A.G. Nusbaum, A. Sawaya, S.B. Patel, L. Khalid, R.R. Isseroff, M. Tomic-Canic. Epithelialization in Wound Healing: A Comprehensive Review. Adv. Wound. Care (New Rochelle). 3(7) (2014) 445-464 doi: 10.1089/wound.2013.0473.
18. Y. R.Kim, B.Nam, A. R.Han, J.B. Kim, C.H. Jin, Isoegomaketone from *Perilla frutescens* (L.) Britt Stimulates MAPK/ERK Pathway in Human Keratinocyte to Promote Skin Wound Healing *Evid. Based Complementary Altern. Med.* (2021) 6642606. <https://doi.org/10.1155/2021/6642606>
19. H. Kobayashi, S. Aiba, Y. Yoshino, H. Tagami, Acute cutaneous barrier disruption activates epidermal p44/42 and p38 mitogen-activated protein kinases in human and hairless guinea pig skin. Exp. Dermatol. 12(6) (2003) 734–746. DOI: [10.1111/j.0906-6705.2003.00045.x](https://doi.org/10.1111/j.0906-6705.2003.00045.x)
20. S.Lee, M.S. Kim, S.J. Jung, D. Kim, H.J. Park, D. Cho, ERK activating peptide, AES16-2M promotes wound healing through accelerating migration of keratinocytes. Sci Rep. 8(1) (2018)14398. doi: 10.1038/s41598-018-32851-y.
21. J.Cursons, J.Gao, D.G.Hurley, C.G.Print, P.R.Dunbar, M.D.Jacobs, E.J.Crampin, Regulation of ERK-MAPK signaling in human epidermis. BMC Syst.Biol. 9 (2015) 41. <https://doi.org/10.1186/s12918-015-0187-6>

22. R.K.Sivamani ,C.E. Pullar ,C.G. Manabat-Hidalgo ,D.M. Roche ,R.C. Carlsen , et al.  
**Stress-Mediated Increases in Systemic and Local Epinephrine Impair Skin Wound Healing: Potential New Indication for Beta Blockers** Plos Med. 6(1) (2009) e1000012. <https://doi.org/10.1371/journal.pmed.1000012>
23. Luqman, A. Götz, F. The Ambivalent Role of Skin Microbiota and Adrenaline in Wound Healing and the Interplay between Them. *Int. J. Mol. Sci.* 22 (2021) 4996. <https://doi.org/10.3390/ijms22094996>
24. S. Choi, M.Yoon, K.Y.Choi, [Approaches for Regenerative Healing of Cutaneous Wound with an Emphasis on Strategies Activating the Wnt/ \$\beta\$ -Catenin Pathway](#) Adv. Wound Care (New Rochelle) 11(2) (2022) 70-86 <https://doi.org/10.1089/wound.2020.1284>
25. K. S.Houschyar, A.Momeni, M. N.Pyles, Z. N. Maan, A. J.Whittam, F.Siemers, Wnt signaling induces epithelial differentiation during cutaneous wound healing. *Organogenesis*. 11(3) (2015) 95-104. doi: 10.1080/15476278.2015.1086052.
26. H.Zhang, X. Nie, X. Shi, J. Zhao, Y. Chen, Q. Yao, C. Sun, J. Yang. Regulatory Mechanisms of the Wnt/ $\beta$ -Catenin Pathway in Diabetic Cutaneous Ulcers. *Front Pharmacol.* 9 (2018) 1114. doi: 10.3389/fphar.2018.01114.
27. J.Luke, P.Fulcher, S.Gopal, Functions and regulation of the serine/threonine protein kinase CK1 family: moving beyond promiscuity. *Biochem.J* 477(23) (2020) 4603–4621. doi: <https://doi.org/10.1042/BCJ20200506>
28. R.A.I Reshad, S.Alam, H.B. Raihan, K.N. Meem, F. Rahman, F. Zahid, M.I.Rafid, S.MO.Rahman, S.Omit, M.H.Ali, In silico investigations on curcuminoids from *Curcuma longa* as positive regulators of the Wnt/ $\beta$ -catenin signaling pathway in wound healing. *Egypt J. Med. Hum. Genet.* 22(65) (2021). <https://doi.org/10.1186/s43042-021-00182-9>
29. LF. Ng, P.Kaur, N. Bunnag, J. Suresh, I.C.H. Sung, Q.H. Tan, J. Gruber, N.S. Tolwinski, WNT Signaling in Disease. *Cells.* 8(8) (2019) 826. doi: 10.3390/cells8080826.

30. S.Rennoll, G. Yochum, Regulation of MYC gene expression by aberrant Wnt/ $\beta$ -catenin signaling in colorectal cancer. *World J. Biol. Chem.* 6(4) (2015) 290-300. doi: 10.4331/wjbc.v6.i4.290.
31. B.T.MacDonald, X. He, Frizzled and LRP5/6 receptors for Wnt/ $\beta$ -catenin signaling. *Cold Spring Harb. Perspect. Biol.* 4(12) (2012) doi: 10.1101/cshperspect.a007880.
32. B.T.MacDonald, K. Tamai, X. He, Wnt/beta-catenin signaling: components, mechanisms, and diseases. *Dev. Cell.* 17(1) (2009) 9-26. doi: 10.1016/j.devcel.2009.06.016.
33. K.Willert, S. Shibamoto, R. Nusse, Wnt-induced dephosphorylation of axin releases beta-catenin from the axin complex. *Genes Dev.* 13(14) (1999)1768-73. doi: 10.1101/gad.13.14.1768.
34. L. Yuangang, M. K.Martin, p53 protein at the hub of cellular DNA damage response pathways through sequence-specific and non-sequence-specific DNA binding, *Carcinogenesis*, 22(6) (2001) 851–860, <https://doi.org/10.1093/carcin/22.6.851>
35. L. Rong , G. J. Hannon, D.Beach, B. Stillman, Subcellular distribution of p21 and PCNA in normal and repair-deficient cells following DNA damage. *Curr. Biol.* 6 (1996) 189-199.[https://doi.org/10.1016/S0960-9822\(02\)00452-9](https://doi.org/10.1016/S0960-9822(02)00452-9)
36. S. Maurya, V.K. Chitti, S.V. Kabir, R. Shanker, K. Nayak, D. Khurana, Manchanda, R.K. Gadugu, S. Kumar, V, Wound Healing Activity of a Novel Formulation SKRIN via Induction of Cell Cycle Progression and Inhibition of PCNA–p21 Complex Interaction Leading to Cell Survival and Proliferation. *ACS Pharmacol. Transl. Sci.* 4 (2021) 352–364. DOI:10.1021/acsptsci.0c00209
37. D.Jiang, V.C. de Vries, J. Muschhammer, S. Schatz, H. Ye, T. Hein, M. Fidan, V.S.Romanov, Y.Rinkevich, K. Scharffetter-Kochanek, Local and transient inhibition of p21 expression ameliorates age-related delayed wound healing. *Wound Repair Regen.* 28 (2020) 49–60.
38. X.Chen, W.Zhang ,Y.F Gao. X.Q.Su, Z.H.Zhai, Senescence-like changes induced by expression of p21Waf1/Cip1 in NIH3T3 cell line. *Cell Res* 12 (2002) 229–233 <https://doi.org/10.1038/sj.cr.7290129>.

39. C.Cayrol, M. Knibiehler, B. Ducommun, p21 binding to PCNA causes G1 and G2 cell cycle arrest in p53-deficient cells. *Oncogene*. 6(3) (1998) 311-20. doi: 10.1038/sj.onc.1201543.
40. T. Abbas, A. Dutta, p21 in cancer: intricate networks and multiple activities. *Nat. Rev. Cancer*. 9(6) (2009) 400-14. doi: 10.1038/nrc2657.
41. M.J.Reiss, Y.P. Han, E. Garcia, M. Goldberg, H. Yu, W.L. Garner. Matrix metalloproteinase-9 delays wound healing in a murine wound model. *Surgery*. 47(2) (2010) 295-302. doi: 10.1016/j.surg.2009.10.016.
42. T.T. Nguyen, S.Mobashery, M.Chang, Roles of Matrix Metalloproteinases in Cutaneous Wound Healing. *InTech*. (2016). doi: 10.5772/64611.
43. M.Gooyit, Z. Peng, W.R.Wolter, H. Pi, D. Ding, D. Hesek, M. Lee, B.Bogges, M. Champion, M.A.Suckow, Mobashery, S, M.Chang, A chemical biological strategy to facilitate diabetic wound healing. *ACS Chem. Biol*. 9(1) (2014) 105–110. <https://doi.org/10.1021/cb4005468>
44. M.Gao, T.T. Nguyen, M.A. Suckow, W.R. Wolter, M. Gooyit, S. Mobashery, M. Chang, Acceleration of diabetic wound healing using a novel protease-anti-protease combination therapy. *Proc. Natl. Acad. Sci. U S A*. 112(49) (2015)15226–15231.
45. M.P.Caley, V.L. Martins, E.A. O'Toole . Metalloproteinases and Wound Healing. *Adv. Wound Care* (New Rochelle). 4(4) (2015) 225-234. doi: 10.1089/wound.2014.0581.
46. G.A.Cabral-Pacheco, I. Garza-Veloz ,C. Castruita-De la Rosa ,J.M. Ramirez-Acuña , B.A.Perez-Romero, J.F. Guerrero-Rodriguez ,N. Martinez-Avila ,M.L. Martinez-Fierro . The Roles of Matrix Metalloproteinases and Their Inhibitors in Human Diseases. *Int. J. Mol. Sci*. 21(24) (2020) 9739. doi: 10.3390/ijms21249739.

47. R. H.Yang, S. H.Qi., B.Shu, S.B.Ruan, Z.P.Lin, Y.Lin, R.Shen, F.G.Zhang, X.D.Chen, J.L.Xie, Epidermal stem cells (ESCs) accelerate diabetic wound healing via the Notch signalling pathway. *Biosci. Rep.* 36(4) (2016) e00364. doi: <https://doi.org/10.1042/BSR20160034>
  
48. V.G.Sunkari, New pathogenic mechanisms in diabeteic wound healing Karolinska Institutet, Stockholm (2012) 14-18.
  
49. X.Zheng, S.Narayanan, V.G. Sunkari, S. Eliasson, I.R. Botusan, J. Grünler, A.I. Catrina, F.Radtke, C. Xu, A.Zhao, N.R. Ekberg, U. Lendahl, S.B. Catrina, Triggering of a Dll4-Notch1 loop impairs wound healing in diabetes. *Proc. Natl. Acad. Sci. U S A.* 116(14) (2019) 6985-6994. doi: 10.1073/pnas.1900351116.
  
50. F.Begum,R. Keni, T.N.Ahuja, F.Beegum, K.Nandakumar, R.R.Shenoy, Notch signaling: A possible therapeutic target and its role in diabetic foot ulcers. *Diabetes Metab Syndr.* 16(7) (2022)102542. doi: 10.1016/j.dsx.2022.102542.
  
51. O.Krizanova, A. Penesova, J. Sokol, A. Hokynkova, A. Samadian, P. Babula, Signaling pathways in cutaneous wound healing. *Front. Physiol.* 13 (2022) 1030851. doi: 10.3389/fphys.2022.1030851.
  
52. P.Kolimi, S. Narala, D. Nyavanandi, A.A.A. Youssef, N. Dudhipala, Innovative Treatment Strategies to Accelerate Wound Healing: Trajectory and Recent Advancements. *Cells.* 11(15) (2022) 2439. doi: 10.3390/cells11152439.
  
53. S.C.Kim ,J.H. Lee, M.H. Kim, J.A. Lee, Y.B. Kim, E. Jung, Y.S. Kim, J. Lee, D. Park, Hordenine, a single compound produced during barley germination, inhibits melanogenesis in human melanocytes. *Food Chem.* 41(1) (2013) 174-81. doi: 10.1016/j.foodchem.2013.03.017.

54. J. Priscilla, D.A. Dhas, I.H. Joe, S. Balachandran, Spectroscopic, electron localization function, chemical reactivity and antihypertensive activity study on hordenine alkaloid by density functional theory approach, J Mol Struct, 1229 (2021) 129823, <https://doi.org/10.1016/j.molstruc.2020.129823>.
55. Vishvakrama P, Sharma S. Liposomes: an overview. Journal of Drug Delivery and Therapeutics. 2014 Jun 24:47-55.
56. Vishvakarma P. Design and development of montelukast sodium fast dissolving films for better therapeutic efficacy. Journal of the Chilean Chemical Society. 2018 Jun;63(2):3988-93.
57. Vishvakarma P, Mandal S, Verma A. A review on current aspects of nutraceuticals and dietary supplements. International Journal of Pharma Professional's Research (IJPPR). 2023;14(1):78-91.
58. Prabhakar Vishvakarma, Jaspreet Kaur, Gunosindhu Chakraborty, Dhruv Kishor Vishwakarma, Boi Basanta Kumar Reddy, Pampayya Thanthathi, Shaik Aleesha, Yasmin Khatoon. Nephroprotective Potential of Terminalia Arjuna Against Cadmium-Induced Renal Toxicity by In-Vitro Study. J. Exp. Zool. India Vol. 28, No. 1, pp. 939-944, 2025
59. Prabhakar V, Agarwal S, Chauhan R, Sharma S. Fast dissolving tablets: an overview. International Journal of Pharmaceutical Sciences: Review and Research. 2012;16(1):17.
60. Mandal S, Vishvakarma P, Verma M, Alam MS, Agrawal A, Mishra A. Solanum Nigrum Linn: an analysis of the Medicinal properties of the plant. Journal of Pharmaceutical Negative Results. 2023 Jan 1:1595-600.
61. Vishvakarma P, Mandal S, Pandey J, Bhatt AK, Banerjee VB, Gupta JK. An Analysis Of The Most Recent Trends In Flavoring Herbal Medicines In Today's Market. Journal of Pharmaceutical Negative Results. 2022 Dec 31:9189-98.
62. Mandal S, Vishvakarma P, Mandal S. Future Aspects And Applications Of Nanoemulgel Formulation For Topical Lipophilic Drug Delivery. European Journal of Molecular & Clinical Medicine. 2023;10(01):2023.
63. Mandal S, Vishvakarma P. Nanoemulgel: A Smarter Topical Lipidic Emulsion-based Nanocarrier. Indian J of Pharmaceutical Education and Research. 2023;57(3s):s481-98.

64. Prabhakar V, Agarwal S, Chauhan R, Sharma S. Fast dissolving tablets: an overview. International Journal of Pharmaceutical Sciences: Review and Research. 2012;16(1):17S. Q. Pantaleão, P. O. Fernandes, J. E. Gonçalves, V. G. Maltarollo, K. M. Honorio, Predicting ADMET properties before subjecting the compound to resource intensive preclinical and clinical studies is very important to avoid failure of drug in later stages. ChemMedChem 17 (2022) e202100542.
65. Drug Discovery and ADMET process: A Review Dr. Preeti Sagar Patil Int.J.Adv.Res.Biol.Sci. 3(7) (2016) 181-192 <http://s-o-i.org/1.15/ijarbs-2016-3-7-26>
66. D. Antoine, O. Michielin, V. Zoete. S. ADME: a free web tool to evaluate pharmacokinetics, drug likeness and medicinal chemistry friendliness of small molecules. Sci Rep. 7 (2017) 42717.1-13 doi: 10.1038/srep42717.
67. S.Salentin, S. Schreiber, V.J. Haupt, M.F. Adasme, M. Schroeder, PLIP: fully automated protein-ligand interaction profiler. Nucleic Acids Res. 43(W1) (2015) W443-7. doi: 10.1093/nar/gkv315.
68. R. Salomon-Ferrer, D.A. Case, R.C. Walker. An overview of the Amber biomolecular simulation package. WIREs Comput. Mol. Sci. 3 (2013) 198-210
69. B. Webb, A. Sal, Comparative Protein Structure Modeling Using Modeller. Current Protocols in Bioinformatics 54, John Wiley & Sons, Inc., (2016).5.6.1-5.6.37
70. B.R. Miller III , T. D. McGee Jr , J. M. Swails, N. Homeyer, H. Gohlke, and A. E. Roitberg, MMPBSA.py: An Efficient Program for End-State Free Energy Calculations J. Chem. Theory Comput. 8 (9) (2012) 3314-3321 DOI: 10.1021/ct300418h
71. Z.Xu, Q. Zhang, C. Ding, F. Wen, F. Sun, Y. Liu, C. Tao, J. Yao, Beneficial Effects of Hordenine on a Model of Ulcerative Colitis. Molecules. 28(6) (2023) 2834. doi: 10.3390/molecules28062834.

72. J.W.Zhou, H.Z.Luo, H.Jiang, T.K.Jian,Z.Q.Chen,A.Q.Jia, Hordenine: A Novel Quorum Sensing Inhibitor and Antibiofilm Agent against *Pseudomonas aeruginosa* J Agric Food Chem. 66 (7) (2018) 1620-1628 DOI: 10.1021/acs.jafc.7b05035
  
73. H.J. Hapke, W.Strathmann, Pharmacological effects of Hordenine. Dtsch Tierärztl Wochenschr 102 (1995) 228-232
  
74. M.Hahn, V. Lindemann, M. Behrens, D. Mulac, K. Langer, M. Esselen, H.U.Humpf Permeability of dopamine D2 receptor agonist hordenine across the intestinal and blood-brain barrier *in vitro*. PLoS ONE 17(6) (2022) e0269486.  
<https://doi.org/10.1371/journal.pone.0269486>
  
75. C.R.M. Souza, W.P.Bezerra, J.T.Souto, Marine Alkaloids with Anti-Inflammatory Activity: Current Knowledge and Future Perspectives. Mar Drugs. 18(3) (2020) 147 doi: 10.3390/md18030147.
  
76. X.Zhang, L. Du, J.Zhang, C. Li, J. Zhang, X. Lv, Hordenine Protects Against Lipopolysaccharide-Induced Acute Lung Injury by Inhibiting Inflammation. Front Pharmacol. 12 (2021) 712232. doi: 10.3389/fphar.(2021).712232.
  
77. S.Su, M. Cao, G.Wu, Z. Long , X. Cheng , J. Fan, Z. Xu, H. Su, Y. Hao, G. Li, J. Peng , S.Li , X. Wang, Hordenine protects against hyperglycemia-associated renal complications in streptozotocin-induced diabetic mice. Biomed Pharmacother. 104 (2018)315-324. doi: 10.1016/j.biopha.2018.05.036.
  
78. J.I. Jones, TT.Nguyen, Z. Peng, M. Chang, Targeting MMP-9 in Diabetic Foot Ulcers. *Pharmaceuticals*. 12(2) (2019) 79. <https://doi.org/10.3390/ph12020079>

79. S. Chadwick, R. Heath, M. Shah, Abnormal pigmentation within cutaneous scars: A complication of wound healing. *Indian J. Plast. Surg.* 45(2) (2012) 403–411. doi: 10.4103/0970-0358.101328.
80. H.J. Zhu, M. Fan , W. Gao . Identification of potential hub genes associated with skin wound healing based on time course bioinformatic analyses. *BMC Surg.* (2021) Jun 30;21(1):303. doi: 10.1186/s12893-021-01298-w.
81. S.Y. Lee, KJ. Won, DY. Kim, M.J. Kim, Y.R. Won, N.Y. Kim, H.M. Lee, Wound Healing-Promoting and Melanogenesis-Inhibiting Activities of *Angelica polymorpha* Maxim. Flower Absolute In Vitro and Its Chemical Composition. *Molecules.* 26(20) (2021) 6172. doi: 10.3390/molecules26206172.
82. G.A. Patani , E.J. LaVoie, Bioisosterism: A Rational Approach in Drug Design. *Chem. Rev.* 96(8) (1996) 3147–3176 doi: 10.1021/cr950066q.
83. S.R. Langdon, P. Ertl, N. Brown, Bioisosteric Replacement and Scaffold Hopping in Lead Generation and Optimization. *Mol Inform.* 29(5) (2010) 366-85 doi: 10.1002/minf.201000019.
84. N. Brown, Bioisosteres and Scaffold Hopping in Medicinal Chemistry. *Mol Inform.* (2014) 33(6-7) 458-62. doi: 10.1002/minf.201400037.
85. D.Alexej, S. Cocklin, "Bioisosteric Replacement as a Tool in Anti-HIV Drug Design" *Pharmaceuticals* 13(3) (2020) 36 doi: 10.3390/ph13030036.
86. O. Bobiļeva, R. Bobrovs, I. Kaņepe, L. Patetko, G. Kalniņš, M. Šišovs, A.L. Bula, S.GriNberga, M.R. Borodušķis, A. Ramata-Stunda, N. Rostoks, A. Jirgensons, K. Ta Rs, K. Jaudzems, Potent SARS-CoV-2 mRNA Cap Methyltransferase Inhibitors by

Bioisosteric Replacement of Methionine in SAM Cosubstrate. ACS Med Chem Lett. 12(7) (2021) 1102-1107. <https://doi.org/10.1021/acsmchemlett.1c00140>

87. P.A.M.Jansen, D.A.van der Krieken, P.N.M.Botman, R.H.Blaauw, L.Cavina, E.M.Raaijmakers, E.de Heuvel,J.Sandrock,L.J.Pennings P.H.H. Hermkens,P.L.J.M. Zeeuwen, F.P.J.T.Rutjes, J.Schalkwijk, Stable pantothenamide bioisosteres: novel antibiotics for Gram-positive bacteria. J Antibiot (Tokyo). 72(9) (2019) 682-692. doi: 10.1038/s41429-019-0196-6.
88. [Tijjani. H](#), [Olatunde. A](#), A. P. [Adegunloye](#), A.A.[Ishola](#), In silico insight into the interaction of 4-aminoquinolines with selected SARS-CoV-2 structural and nonstructural proteins, In Drug Discovery Update, Coronavirus Drug Discovery,Elsevier, 3 (2022) 313-333 <https://doi.org/10.1016/B978-0-323-95578-2.00001-7>.
89. M.M.da Silva, M.Comin, T.S.Duarte, M.A.Foglio, J.E.de Carvalho, M.C.do Vieira, A.S.Formagio, Synthesis, antiproliferative activity and molecular properties predictions of galloyl derivatives. Molecules. 20(4) (2015) 5360-73. doi: 10.3390/molecules20045360.
90. K. Palm, P. Stenberg, K. Luthman, P. Artursson, Polar molecular surface properties predict the intestinal absorption of drugs in humans Pharm. Res. 14(5) (1997) 568– 571 doi: 10.1023/a:1012188625088.
91. H.Pajouhesh, G.R. Lenz, Medicinal chemical properties of successful central nervous system drugs. NeuroRx. 2(4) (2005) 541-53. doi: 10.1602/neurorx.2.4.541.
92. O. Ursu, A. Rayan,A. Goldblum, T.Oprea, Understanding drug-likeness, Wiley Interdiscip. Rev. Comput. Mol.1(5) (2011) 760 – 781 DOI:[10.1002/wcms.52](https://doi.org/10.1002/wcms.52)

93. D. Ranjith, C. Ravikumar, SwissADME predictions of pharmacokinetics and drug-likeness properties of small molecules present in Ipomoea mauritiana Jacq J Pharmacogn Phytochem 8(5) (2019) 2063-2073
  
94. D.F.Veber, S.R. Johnson, H.Y. Cheng, B.R. Smith, K.W. Ward, K.D. Kopple, Molecular properties that influence the oral bioavailability of drug candidates. J Med Chem. 45(12) (2002) 2615-23. doi: 10.1021/jm020017n.
  
95. A. Zerroug, S. Belaidi, I.B.Brahim, L. Sinha, S. Chtita, Virtual screening in drug-likeness and structure/activity relationship of pyridazine derivatives as Anti-Alzheimer drugs, J King Saud Univ Sci.31(4) (2019) 595-601, <https://doi.org/10.1016/j.jksus.2018.03.024>.
  
96. R.S.Porto, L.F.de Lima Costa, V.A.Porto Identification of Synthetic 2-Mercaptobenzimidazole Derivatives as Inhibitors of Spike Protein of SARS-CoV-2 by Virtual Screening Lett.Appl. Nanobioscience 12(2) (2023), 31 <https://doi.org/10.33263/LIANBS122.031>
  
97. J. Bojarska, M. Remko, M. Breza, I.D. Madura, K. Kaczmarek, J. Zabrocki, W.M. Wolf, A Supramolecular Approach to Structure-Based Design with A Focus on Synthons Hierarchy in Ornithine-Derived Ligands: Review, Synthesis, Experimental and in Silico Studies. *Molecules*( 2020), 25, 1135. <https://doi.org/10.3390/molecules25051135>
  
98. F.J. Sharom, The P-glycoprotein multidrug transporter. *Essays Biochem.* 50(1) (2011) 161–78. doi: 10.1042/bse0500161.
  
99. J.H.Lin, M.Yamazaki, Role of P-glycoprotein in pharmacokinetics: clinical implications. *Clin Pharmacokinet.* 42(1) (2003) 59–98. doi: 10.2165/00003088-200342010-00003.

100. M.L.Amin, P-glycoprotein Inhibition for Optimal Drug Delivery. *Drug Target Insights*. 7 (2013) 27-34. doi: 10.4137/DTI.S12519
101. C. Karthika, R. Sureshkumar, P-Glycoprotein Efflux Transporters and Its Resistance Its Inhibitors and Therapeutic Aspects. *IntechOpen*. (2021) doi: 10.5772/intechopen.90430
102. W. Zhang ,Y. Han ,S.L. Lim ,L.Y. Lim . Dietary regulation of P-gp function and expression. *Expert Opin Drug Metab Toxicol*. 5(7) (2009) 789-801 doi: 10.1517/17425250902997967.
103. D.P. Bezerra ,F.O. de Castro ,A.P. Alves ,C. Pessoa ,M.O. de Moraes ,E.R. Silveira , M.A.Lima, F.J.Elmiro, N.M.de Alencar, R.O. Mesquita, M.W.Lima, L.V.Costa-Lotufo, In vitro and in vivo antitumor effect of 5-FU combined with piplartine and piperine. *J. Appl. Toxicol*. 28(2) (2008) 156-163 doi: 10.1002/jat.1261.
104. T. Nabekura,S. Kamiyama, S. Kitagawa, Effects of dietary chemopreventive phytochemicals on P-glycoprotein function. *Biochem. Biophys. Res. Commun*. 327(3) (2005) 866-870 doi: 10.1016/j.bbrc.2004.12.081.
105. T.Nabekura, Overcoming multidrug resistance in human cancer cells by natural compounds. *Toxins*, 2(6) (2010) 1207–1224. <https://doi.org/10.3390/toxins2061207>
106. Y.L. Han, H.L.Yu,D. Li,X.L. Meng,Z.Y. Zhou,Q. Yu,X.Y. Zhang,F.J. Wang, C.Guo, Inhibitory effects of limonin on six human cytochrome P450 enzymes and P-glycoprotein in vitro. *Toxicol. In Vitro*.25(8) (2011) 1828-1833 doi: 10.1016/j.tiv.2011.09.023.

107. M. Zhao, J. Ma, M. Li, Y. Zhang, B. Jiang, X. Zhao, C. Huai, L. Shen, N. Zhang, L. He, S. Qin, Cytochrome P450 Enzymes and Drug Metabolism in Humans. *Int. J. Mol. Sci.* 22(23) (2021)12808. doi: 10.3390/ijms222312808.
108. U.M.Zanger, M.Schwab, Cytochrome P450 enzymes in drug metabolism: Regulation of gene expression, enzyme activities, and impact of genetic variation, *Pharmacol. Ther.* 138(1) (2013) 103-141, <https://doi.org/10.1016/j.pharmthera.2012.12.007>.
109. J. Hakkola, J. Hukkanen, M. Turpeinen, O. Pelkonen, Inhibition and induction of CYP enzymes in humans: an update. *Arch. Toxicol.* 94 (2020) 3671–3722 <https://doi.org/10.1007/s00204-020-02936-7>
110. J. Ziemska, J. Solecka, M. Jarończyk, In Silico Screening for Novel Leucine Aminopeptidase Inhibitors with 3,4-Dihydroisoquinoline Scaffold. *Molecules* 25 (2020) 1753. <https://doi.org/10.3390/molecules25071753>
111. M. Garcial, V. Buwa, *In Silico* ADME Analysis And Molecular Docking Applied To Flavonoids To Find Drug Lead Compounds Targeting DRD4 *Innovare Journal of Medical Science*, 10(4) (2022) 21-27
112. H.I. Umar, A. Ajayi, R.O. Bello, H.O. Alabere, A.A. Sanusi, O.O. Awolaja, M.M. Alshehri, P.O. Chukwuemeka, Novel Molecules derived from 3-O-(6-galloylglucoside) inhibit Main Protease of SARS-CoV 2 In Silico. *Chem. Pap.* **76** (2022) 785–796 <https://doi.org/10.1007/s11696-021-01899-y>
113. P. Ertl, A. Schuffenhauer, Estimation of synthetic accessibility score of drug-like molecules based on molecular complexity and fragment contributions *J. Cheminform* **1** (2009). 8 <https://doi.org/10.1186/1758-2946-1-8>

114. N. Kochev, S. Avramova, P. Angelov, N.Jeliazkova, Computational Prediction of Synthetic Accessibility of Organic Molecules with Ambit-Synthetic Accessibility Tool. Org. Chem. Ind. J. 14(2) (2018) 123
115. S. Scheler, A. Fahr, X. Liu, Linear combination methods for prediction of drug skin permeation. ADMET & DMPK 2(4) (2015) 199–220 <https://doi.org/10.5599/admet.2.4.147>
116. D.A. Omoboyowa, Sterols from Jatropha tanjorensis leaves exhibit anti-inflammatory potential: in vitro and in silico studies Bull. Natl. Res. Cent. 45 (2021)194 <https://doi.org/10.1186/s42269-021-00658-z>
117. R.G. Tirona, R.B. Kim, Introduction to clinical pharmacology In: Clinical and translational science (2nd Edn): Academic press. USA, (2017) 365–388
118. S.F. Zhou, Drugs behave as substrates, inhibitors and inducers of human cytochrome P450 3A4. Curr Drug Metab 9(4) (2008) 310-22 doi: 10.2174/138920008784220664.
119. G.Ayano, Psychotropic Medications Metabolized by Cytochromes P450 (CYP) 3A4 Enzyme and Relevant Drug Interactions:Review of Articles Austin J. Psychiatry Behav. Sci. 3(2) 2016 1054.
120. M. Rahman, J.J. Browne, J. Van Crugten, M.F. Hasan, L. Liu, B.J. Barkla, In Silico, Molecular Docking and In Vitro Antimicrobial Activity of the Major Rapeseed Seed Storage Proteins. Front Pharmacol. 11 (2020)1340. <https://doi.org/10.3389/fphar.2020.01340>
121. H. L. B. Braz, J. A. M. Silveira, A. D. Marinho, M. E. A.de Moraes, M. O. Moraes Filho, H. S. A.Monteiro, R. J. B. Jorge, In silico Study of Azithromycin, Chloroquine and Hydroxychloroquine and their Potential Mechanisms of Action against SARS-CoV-2

- Infection. Int. J. Antimicrob. Agents 56(3) (2020) 106119.  
<https://doi.org/10.1016/j.ijantimicag.2020.106119>
122. M. Batool ,A. Tajammal ,F. Farhat ,F. Verpoort ,Z.A.K. Khattak ,M. Mehr-un-Nisa, Shahid ,H.A. Ahmad ,M.A. Munawar ,M. Zia-ur-Rehman ,M. Asim Raza Basra . Molecular Docking, Computational, and Antithrombotic Studies of Novel 1,3,4-Oxadiazole Derivatives. Int. J. Mol. Sci. 19(11) (2018) 3606 doi: 10.3390/ijms19113606.
123. H.M. Ali, A.G.Soliman, H.G.A.G. Elfiky, SAR and QSAR of COVID-19 Main Protease–Inhibitor Interactions of Recently X-ray Crystalized Complexes. Proc. Natl. Acad. Sci., India, Sect. B Biol. Sci. 92 (2022). 281–291 doi: 10.1007/s40011-021-01338-8.
124. V. Umashankar, S.H. Deshpande, H.V. Hegde, I.Singh, D. Chattopadhyay, Phytochemical Moieties from Indian traditional medicine for targeting dual hotspots on SARS-CoV-2 spike protein: an integrative in-silico approach. Front. Med. 8 (2021) doi: 10.3389/fmed.2021.672629.
125. T. Lippert , M. Rarey, Fast automated placement of polar hydrogen atoms in protein-ligand complexes. J. Cheminform. 1 (2009) 13. <https://doi.org/10.1186/1758-2946-1-13>
126. Davis MI, Hunt JP, Herrgard S, Ciceri P, Wodicka LM, Pallares G, Hocker M, Treiber DK, Zarrinkar PP. (2011) Comprehensive analysis of kinase inhibitor selectivity. *Nat Biotechnol*, 29 (11): 1046-51. [PMID:[22037378](https://pubmed.ncbi.nlm.nih.gov/22037378/)]
- Wodicka LM, Ciceri P, Davis MI, Hunt JP, Floyd M, Salerno S, Hua XH, Ford JM, Armstrong RC, Zarrinkar PP *et al.*. (2010) Activation state-dependent binding of small molecule kinase inhibitors: structural insights from biochemistry. *Chem Biol*, 17 (11): 1241-9. [PMID:[21095574](https://pubmed.ncbi.nlm.nih.gov/21095574/)]